# FINITE ELEMENT ANALYSIS OF A BEAM WITH CORRUGATED WEB OF A JIB CRANE

## A Thesis

***Submitted in partial fulfillment of the requirements for the award of the degree***

***Of***

**MASTER OF TECHNOLOGY**

**IN**

**CIVIL ENGINEERING**

**With specialization in**

**STRUCTURAL ENGINEERING**

***Under the supervision of***

**Dr. Saurav**
**(Assistant Professor)**

***by***

**DAMINI TALWAR**
**Roll No. 162660**

**To**

**JAYPEE UNIVERSITY OF INFORMATION TECHNOLOGY**

**WAKNAGHAT, SOLAN – 173234**

**HIMACHAL PRADESH, INDIA**

**May 2018**

# CERTIFICATE

This is to certify that the work which is being presented in the thesis titled **“Finite Element Analysis of a beam with corrugated web of a Jib Crane”** in partial fulfillment of the requirements for the award of the degree of Master of Technology in Civil Engineering with specialization in “Structural Engineering” and submitted to the Department of Civil Engineering, Jaypee University of Information Technology, Waknaghat is an authentic record of work carried out by Damini Talwar (162660) during a period from July 2017 to May 2018 under the supervision of **Dr. Saurav,** Assistant Professor, Department of Civil Engineering, Jaypee University of Information Technology, Waknaghat.

The above statement made is correct to the best of our knowledge.

Date: - ………………………

| | | |
|---|---|---|
| Dr. Ashok Kumar Gupta | Dr. Saurav | External Examiner |
| Professor & Head of Department | Assistant Professor | |
| Department of Civil Engineering | Department of Civil Engineering | |
| JUIT, Waknaghat | JUIT, Waknaghat | |

ACKNOWLEDGEMENT

I take this opportunity to acknowledge all who have been a great sense of support and inspiration throughout the thesis work. First of all I would like to thank almighty God, my parents and my friends who inspired me and helped, worked for me in every possible way to provide the details about various related topics thus making thesis and report work success. My gratitude goes to our Head of the Department **Prof. (Dr.) Ashok Kumar Gupta** for his guidance, encouragement and support.

I am very grateful to **Dr. Saurav,** Assistant Professor for all his diligence, guidance, encouragement and help throughout the period of thesis, which has enabled me to complete the thesis work in time. I also thank him for the time that he spared for me, from his extreme busy schedule. His insight and creative ideas are always the inspiration for me during the dissertation work.

**Damini Talwar**

**(162660)**

# ABSTRACT

A crane is a machine for lifting and lowering a load and moving it horizontally with the hoisting mechanism being an integral part of the machine. Jib cranes are simplest types and widely used in the small scale industries. A satisfactory design should ensure that the beam of the crane is stable and has enough strength and stiffness against the applied loads. For steel beams having an I-shaped cross section, lateral torsional buckling is a typical mode of instability.

In this study a Jib Crane Boom is analysed on FEM software ANSYS. Conventional plane web cantilever steel I beam S10@25.4lb/feet having a span of 2.54m has been analysed to study the buckling behaviour of the beam under the action of self weight and vertical load at free end. Models are created on AutoCAD and analysed on ANSYS. Buckling load is calculated by using a load multiplier. Further a new design approach of using a web with trapezoidal corrugations has been proposed to study the lateral torsional buckling behaviour of the beam subjected to self weight and vertical load at free end. A total of 32 models with different corrugation angles, web thicknesses and web widths are created and analysed to see the effect of variations in corrugations on the buckling capacity of the beam. From the analysis results, it is also observed that not only web thickness, but also the corrugation plate length, corrugation angle and the corrugation width influence the buckling capacity of the beam. Further the corrugated beam is compared to flat beam on the basis of weight and buckling load and it is observed that corrugated beam is economical and has higher buckling capacity than the flat beam.

**Keywords**: Jib cranes, lateral torsional buckling, finite element analysis.

# TABLE OF CONTENTS

# LIST OF FIGURES

# LIST OF TABLES

# LIST OF ABBREVIATIONS

| | |
|---|---|
| LTB | Lateral torsional buckling |
| FEM | Finite element method |
| ASME | American society of Mechanical engineers |
| CMAA | Crane Manufacturers Association of America |
| LSB | Light steel beam |
| CAD | Computer Aided Design |
| ASTM | American society of testing materials |

`

# CHAPTER 1

# INTRODUCTION

## 1.1 Introduction To Beams And Jib Cranes

### 1.1.1 Beams

Beams are structural members that support loads which are applied transverse to their longitudinal axes. Beams have a far more complex load-carrying action than other structural element such as trusses and cables [13]. Little was known about the exact mechanism by which beams carry loads until recently, relative to the length of time, when such elements were discovered to have been used in early and recent civilizations. The load transfer by a beam is primarily by bending and shear. Any structural member could be considered as a beam if the loads cause bending of the member. If a substantial amount of axial load is also present, the member is referred to as a beam-column [13].

Though some amount of axial effects will be present in any structural member, in several practical solutions, the axial effect can be neglected and the member can be treated as a beam. [13].

However the structural action of a beam is predominantly bending, with other effects such as shear, bearing and buckling also being present [23].

### 1.1.2 Jib Crane

- Today's industry demands versatile, efficient and cost effective equipment while at the same time providing more flexibility along with significant savings through increased productivity. There are several equipment used in industry for material handling, a crane is one of them [8].
- A crane is a mechanical lifting device equipped with a winder, wire ropes and sheaves that can be used both to lift and lower materials and to move them horizontally. It uses one or more simple machines to create mechanical advantage and thus move loads beyond the normal capability of a human [19]. Cranes are commonly employed in the transport industry for the loading and unloading of freight; in the construction industry for the movement of materials; and in the manufacturing industry for the assembling of heavy equipments. It serves a larger area of floor space within its own travelling restrictions than any other permanent type hoisting arrangement [19].

`

- A jib crane is a type of crane making use of a mounted arm to lift and move the material. The arm is mounted either perpendicular to or at an acute angle upwards from a pillar or wall, may rotate along its central axis via a limited arc or possibly a full circle [8].
- A jib crane is in effect a monorail that is cantilevered from its supporting members and pivoted at one end. The horizontal beam provides the track for the hoist trolley. Jib crane have three degrees of freedom. They are vertical, radial, and rotary. However they cannot reach into corners [12].
- Lifting capacity of such cranes may vary from 0.5 ton to 200 ton and outreach from a few meters to 50 meters. Such cranes find various applications in port area, construction site and other outdoor works. For handling general cargo, lifting capacities usually 1.5 ton to 5 ton with maximum out reach of 30 meter [1]. Jib crane provided with grabbing facilities have usually a capacity ranging from 3 ton operating 50 to 100 cycles per hour. Lifting heights may be 30 meter or more [1]. Frequently, these cranes are provided with two main hoisting winches which can be employed singly or together to lift a load [1]. Column mounted jib cranes are commonly used in packaging industry. The size of the crane can be visualized from the height of the operator. These cranes are used for hoisting up to 1 ton loads [1].
- It consists of a pillar fixed to the wall or mounted on the floor. The pillar supports a horizontal jib or boom which has a movable hoist. The hoist is used to lift or lower a load with the help of a drum, or lift-wheel, which has a chain or rope wrapped around it. The drum is driven electrically or pneumatically, and can be operated manually. The lifting medium is usually a chain, although it may also be a fibre rope or wire cable. The load is lifted with the help of a lifting hook attached to the lifting medium.
- The term "jib crane" includes all the cranes that have a rotating boom which is attached to a vertical mast and supports a hoist that operates electrically or pneumatically. Jib cranes are not only preferred in construction business, but also on commercial and military ships.
- Considerable research studies have been carried out about structural and equivalent stresses in order to provide safety under static loading and dynamic behaviour of cranes [25]. Finite element analysis is a powerful technique originally developed for numerical solution of complex problems in structural mechanics, and it remains as a method of choice for complex systems. The basic principal of this numerical method is

`

dividing all the large structure into small elements having simple shapes. The unknown variables of an element are the displacement values for each nodal point [25].

## 1.2 Classification of Jib Crane

Cranes may be classified on the basis of the load carrying capacity, the height to which the load is lifted, and the frequency of lifting the loads [13]. For example, the Crane Manufactures Association of America (CMAA) has classified the cranes as follows [13].

1. Class A1 (standby service)
2. Class A2 (infrequent use)
3. Class B (light service)
4. Class C (moderate service)
5. Class D (heavy duty)
6. Class E (serve duty cycle service)
7. Class F (steel mill)

There are hundreds of jib crane types available, depending on the crane manufacturer. But for the purpose of this blog, which all differ to meet the needs of your operation. In addition, each jib type has its own set of sub-characteristics, and each can be modified for a specific purpose. These make customizing the perfect system for your application easy and efficient. We will look at three common jib cranes [13].

a) Wall-mounted jib

b) Floor-mounted jib

c) Articulating jib

All three jib types can be broken down into specific installation categories and customized to meet your needs.

a) Wall-Mounted Jib Crane, Figure 1.1 - provide 270° rotation for a circular coverage area. With capacities up to 5 tons, these systems are not light weight. However, they are not nearly as heavy-duty as a freestanding system. Wall-mounted jibs require no floor space. There are two main types of wall-mounted jib cranes: cantilever and tie rod supported. The cantilever wall-mounted design offers the greatest amount of clearance above and below the boom. It also transmits less direct force to building columns, making it easy to install on practically any wall or column in your building. The tie rod supported wall-mounted jib crane is extremely economical. It includes no support structure under the boom, so the trolley hoist can easily travel the full length of the boom [13].

`

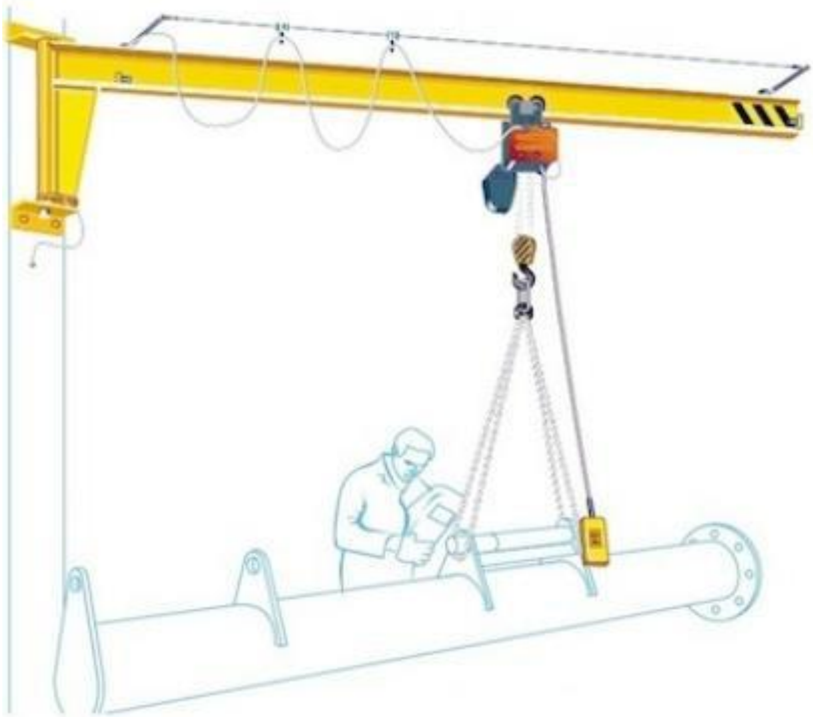

**Figure 1.1:** Wall-mounted Jib Crane [13]

b) Floor Mounted Jib Crane, Figure 1.2 - There are many types of jib cranes under the category of floor-mounted and each serves its own unique purpose. For instance, a freestanding (also known as a *stand-alone*) jib crane is foundation-mounted, which means that it can be installed almost anywhere inside or outside. Freestanding systems offer higher capacities, longer spans, and 360° and 270° rotation to cover a large circular area within your facility. These systems are tough and heavy-duty compared to other floor-mounted types, but they are also more expensive and require a special foundation for proper mounting [13].

`

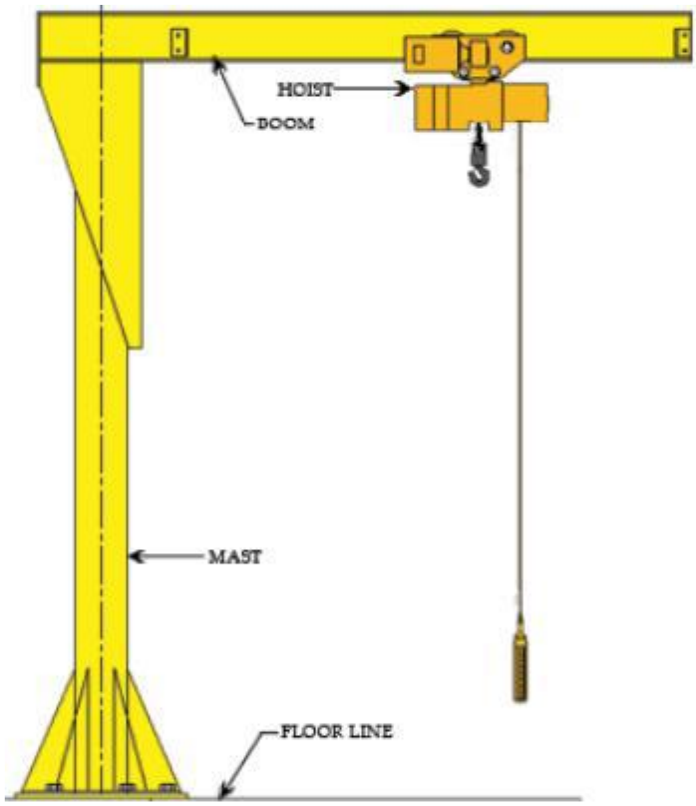


**Figure 1.2:** Floor-mounted Jib crane [13]

This helps to eliminate the cost of a special foundation, which is required for the freestanding system. Mast style jibs are lower cost and can be fully-cantilevered or drop-cantilevered, depending on your facilities overhead structure. The drop cantilever mast style jib crane is almost identical to the full-cantilever system, only it has side-plate connections that allow you to lower the boom at a specified height on the mast. This is extremely useful for facilities that require additional clearance overhead due to obstructions located below the top of the mast. Floor-mounted jib cranes are an excellent option whether they are freestanding or mast mounted depending on the needs of your application [13].

c) Articulating Jib Crane, Figure 1.3 - These versatile material handling solutions are able to lift and move loads around corners and columns, reach into machinery, and service virtually any point between the pivot anchor and the far reach of the boom. They offer multiple installation options, including floor-mounting, wall mounting, ceiling-mounting, and even bridge-mounting. Articulating jib cranes are designed with an inner arm and an outer arm, allowing them to literally articulate around various parts of a facility, in and out of machinery, and over and under practically any other obstruction. The inner arm provides 270° of rotation, while the outer arm provides 360° of rotation

`

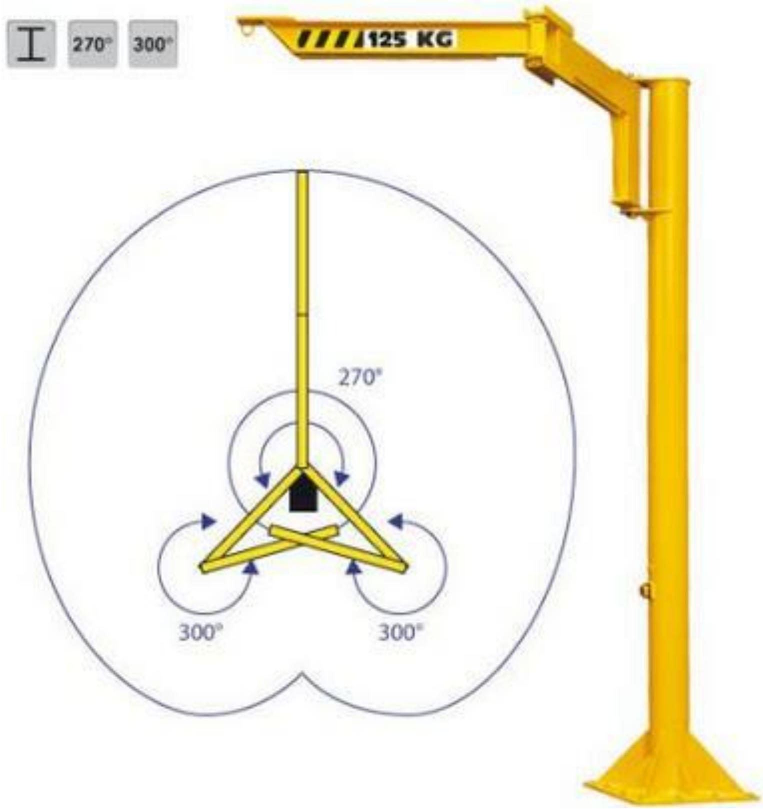


**Figure 1.3:** Articulating Jib crane [13]

With multiple installation types and excellent lift flexibility and range of motion, these systems are a great option for nearly any type of application [13].

## 1.3 Stability Analysis

Stability analysis of a jib crane is required to avoid the accidents that can be caused in case of failure of beam of a jib crane. From studies and investigations, it is observed that the jib crane requires breakdown maintenance most of the times in a year due to the reasons given below [8]:

- Lateral shift of cantilever I-type beam with respect to axis of mounting and because of that movement of trolley is restricted.
- Bending at free end stuck the trolley at tip position.
- Bending caused damage to the beam.

### 1.3.1 Lateral Torsional Buckling

- When an applied load causes both lateral displacement and twisting of a member lateral torsion buckling has occurred.

`

- Lateral torsional buckling may occur in an unrestrained or laterally unsupported beam.
- A beam is considered to be unrestrained when its compression flange is free to displace laterally and rotate [27].

Lateral-buckling is a major design aspect of flexural members of thin walled I-girders. When a slender I-girder is subjected to flexure about its strong axis with insufficient lateral bracing out-of plane bending may occur as applied load approaches its critical value. At this critical value, lateral buckling occurs [15].

Lateral Torsional Buckling is effective on laterally unrestrained beams which are loaded so as to be under bending about their major axis. Calculating the smallest load causing LTB of the beam, which is known as critical LTB load, is a hard problem to solve [15]. Especially for the sections which are under greater warping moments during torsion such as I sections, developing a closed form solution is not practical. Many studies were conducted in search of this solution [16]. The use of corrugated webs is potential method to achieve adequate out-of plane stiffness and shear bulking resistance without using stiffeners. Therefore, further lateral restraints have to be provided to control lateral-buckling using corrugated web [15].

**1.3.2 Purpose of Corrugations:**

To allow the use of thin plates without stiffeners in buildings, bridges construction, crane design, the corrugated webs are introduced. Reduction in beam weight and cost can be achieved because the usage of larger thickness and stiffeners gets eliminated [2]. Providing corrugations in the web considerably reduces the cost of beam fabrication and improves the fatigue life [20].It also improves the aesthetics of structures. There is less literature available on application of corrugated web. The results of available studies indicate that the strength of such girders can be higher as compared to girders with stiffened or un-stiffened web [20]. In present research a web with trapezoidal corrugations is used. In this research the finite element models of plane web as well as corrugated webs are developed and analysis is performed on ANSYS.

`

# CHAPTER 2

# LITERATURE REVIEW

## 2.1 Literature Survey

**Finite element analysis and optimization of Jib Crane Boom: C. C. Dandavatimath and H.D. Sarode [1].**

They investigated the bending of a cantilever I section beam of a jib crane subjected to self weight and load at free end. New designs of web shapes were proposed and analyzed using FEM software ANSYS to see the effect of geometrical parameters on bending and load carrying capacity of the beam. Further results of proposed designs were compared with the conventional beam results. It is observed that with change in web designs load carrying capacity and resistance to bending increases.

**Detail Design and Analysis of a free standing I Beam Jib Crane: M. Dhanoosha and V. Gowtham Reddy [5].**

In this study, a jib crane was designed analytically and was analyzed on FEM software.

Using analytical design dimensions, models are made on CREO and analyzed on ANSYS. Furthermore the stress regions in a floor mounted jib crane were investigated by using 2 different steel i.e. Structural steel and ASME A36 steel. Results were then compared and it is concluded that ASME A36 steel gives less deformation and stress values than Structural steel.

**Effect of Triangular Web Profile on the Shear Behaviour of Steel I-Beam: Fatimah De'nan, Musnira Mustar, Adzhar Bin Hassan and Norbaya Omar [18].**

In this paper a three-dimensional finite element model using LUSAS 14.3 had been made to study the outcome of the steel beam with triangular web shape for the shear buckling behaviour. Beams of different thickness were compared to a normal flat beam. Eigen value buckling analysis was used in calculating the buckling load of the beam with flat web and that with a triangular web shape. Results show that the various web thicknesses gave a significant impact on the shear buckling. Also, the corrugation thickness of the web is also efficient in increasing the shear buckling capacity of the beam.

`

**Design and Analysis with Finite Element Method of Jib Crane: C. I. Gerdemeli, S. Kurt, B. Tasdemir [21].**

In this study a Jib Crane is designed analytically as well as using FEM. Analytical design results and those that were obtained by finite element method have been compared. The consistency of the finite element method for Jib crane design had been looked for. Notably, it has been observed that, FEM is the most practical and efficient method which can be used for Jib crane design. According to the comparison results, it is seen that, the error margins were between the acceptable limits.

**Finite element analysis of jib crane: S.M. Rajmane and A. Jadhav [7].**

In this research work, finite element analysis of a column mounted jib crane was done. Software ANSYS was used for modelling & analysis. During the work, effects of variation of web thickness, web height on deflection of beam & Von Mises stresses were studied. It is found that with an increase in web thickness, deflection and Von Mises stress decrease. With an increase in web height, initially the deflection reduces but later it increases. Von Mises stress also reduces initially, but later increases and becomes constant.

**The Study of Lateral Torsional Buckling Behaviour of Beam with Trapezoid Web Steel Section By Experimental and Finite Element Analysis: Fatimah Denan, M.H. Osman and S. Saad [24].**

In this study experimental and numerical study on lateral torsional buckling behaviour of steel section with trapezoid web were performed. In the experimental work, I sections with dimension 200 x 80 mm and 5 m length were loaded vertically, and were laterally unrestrained to allow lateral torsional buckling to occur. In the analytical study, Eigen-value buckling analysis in the finite element method was performed to determine the critical buckling load of the steel section. Finite element analysis can be used to determine the elastic lateral torsional buckling moment of the steel section. The result shows that corrugation thickness considerably influences the resistance to lateral torsional buckling. Further the results were compared with those of the flat web beam. From the comparison it is concluded that Steel beam with trapezoidal corrugated web have higher resistance to lateral torsional buckling compared to that of steel beam with flat web. Also, sections with higher corrugation thickness have higher resistance to lateral torsional buckling because of higher value of moment of inertia, about minor axis for the section with thicker corrugation.

`

**Jib Crane Analysis using FEM: S.S. Kiranalli and N. U. Patil [10]**.

In this study analysis of a jib crane was done using FEM software ANSYS. Initially the crane was modelled by a simple 2D element as a beam and column, and results were compared with the analytical solutions to check suitability of the mesh and element for 3D model analysis. Further 3D model was created and analyzed on ANSYS to study the effect of change in parameters like web thickness and web heights on maximum deformation and Von Mises stress. It is found that with increase in web thickness and height, the deformation decreases constantly.

**Design and stress analysis of single girder jib crane: R. K. Amreeta and V. Singh [6].**

In this study stress analysis of single girder wall mounted jib crane having load carrying capacity of 1000 kg and a 2.5 m span length and 180 degrees swing range was done.

Different beam sections i.e., MB150, MB125, MB100and 140 × 80 rectangular sections were analysed both analytically and on FEM software ANSYS 14.5. Further, both the FEM and analytical results were compared and the results agreed with each other. From the results it was found that the beam MB 150 is favourable for a wall mounted jib crane of span 2.5m and a load carrying capacity of 1000 kg. Also, it is seen that I section beam has got lesser deformation and stress as compared to rectangular section which makes it suitable in callous climate and in increasing the operating life of the jib. Further it is seen that stresses developed in the beam are smaller than the allowable stress of material of the components, thus the jib crane is safe as per I.S norms IS 807:2006 Design, Erection And Testing, Structural Portion of Cranes and Hoists and IS 15419:2004 Jib Cranes- Code Of Practice.

**Design and analysis of varying cross sectional cantilever beam with trapezoidal web for Jib cranes: Amit S. Chaudhary, Subim N. Khan [8].**

This paper deals with the bending behavior, shear capacity and lateral torsional buckling of I section cantilever beam of a jib crane tested to an eccentric point load and self weight of the beam using Finite element analysis. Different cross sections and different web shaped cantilever beams were proposed in the study. A corrugated trapezoidal web cantilever beam was compared to a flat web cantilever beam. The thickness of flange was kept constant as 10 mm, with span length 5m, 500 kg load lifting capacity for every specimen.

FEA was done on the trapezoidal and straight web section under a load at free end using ANSYS software to examine the effect of the different sectional dimensions such as web thickness, infill length of corrugated plate, width of web and corrugation angle.

`

From the results it is found that trapezoidal web section had offers better resistance to lateral torsional buckling and bending compared to that of a flat web section. Also, high trapezoidal web thickness, large width of web, small length of corrugated plate with web angle 45⁰, 75⁰ results in high resistance to lateral torsional bucking and bending.

**A review paper on design and structural analysis of simply supported gantry crane beam for eccentric loading: Ms Kavita R. Kapadni and S.G. Ganiger [9].**

This paper examines the shear stresses, deflection, lateral torsional buckling in a regular I section simply supported gantry crane beam subjected to a concentrated load at the centre of the beam and the self weight. Since lateral torsional buckling and bending are the important failure modes of a beam they were discussed in the study. Warping and shear centre were also discussed. A design with varying cross sectional shape with trapezoidal web as shown in Figure 2.1 was proposed as an alternative over a regular I section beam to reduce the above mentioned failures.

This study mainly laid emphasis on the most efficient technique to reduce the twisting and lateral torsional buckling of a gantry crane beam by employing different cross sectional shapes of the existing beam. The study demonstrates that for a given load, tapered beam with corrugated trapezoidal web is more resistant to bending, lateral torsional buckling as compared to a normal I section beam. This research will help to reduce the buckling effects usually faced in material handling industries.

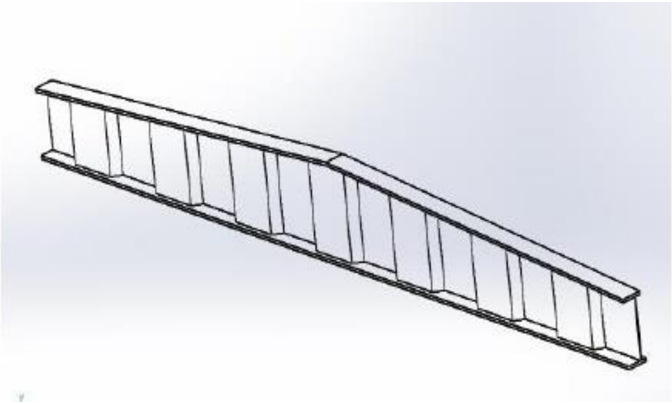

**Figure 2.1:** Tapered beam with corrugated web [9]

`

**Design and Static analysis of I section boom for rotary jib crane: N. S. Khetre, P. S. Bankar, and A. M. Meshram [14].**

In this paper an I section boom was designed for a rotary jib crane. Using Static stress analysis and displacement analysis, yield strength and displacement was calculated analytically for I section. Further the models were made on Solid works and analyzed on COSMOS for stress and displacement and compared with the analytical results. Both the results agreed well with each other.

**Lateral torsional buckling of I-girder with corrugated webs under uniform bending: Jiho Moon, Jong-Won Yi, Byung H. Choi, Hak-Eun Lee [26].**

In this study result of the theoretical and finite element analyses of the lateral–torsional buckling of I-girders with corrugated webs under uniform bending were presented. Further, approximated methods for locating the shear centre and calculating the warping constant of I-girder with corrugated web were proposed. Further it is seen that the lateral–torsional buckling strength of I-girder with corrugated webs under uniform bending can be calculated easily using the proposed methods. A series of finite element analyses were conducted and the results were compared with those of the proposed approximated methods. The results of FEA and approximated methods agreed well and verified the proposed methods. Also, the effects of the corrugation parameters of the web on the lateral–torsional buckling strength of the I-girder with corrugated webs were further discussed in this study. From the results, it is seen that the warping constant of the I-girder with corrugated webs is larger than that of the I-girder with flat webs, while the shear modulus of the corrugated plates is smaller than that of the flat plates.

**Structural Analysis of a cantilever Beam with tapered web section through FEA: Tejal Patil and Nagesh L Shelke [4].**

In this paper twisting anxieties of cantilever steel beam with tapered web were discussed. Beams with different web taperations were dissected and the area and extent of the most extreme bending anxiety were talked about, along with lateral torsional buckling of I beams. FEA was done on a cantilever beam (200mm×100mm with 5m length and vertical load of 500kg) with tapered web section subjected to a point load at the free end and the self weight with the help of ANSYS software. The results were compared to that of cantilever steel beam of same dimensions and same loading conditions having flat web. From the results as shown in Figure 2.2, 2.3 and 2.4 effects of web taperations on bending, lateral torsional buckling, angle of twist, shear and bending stresses were discussed.

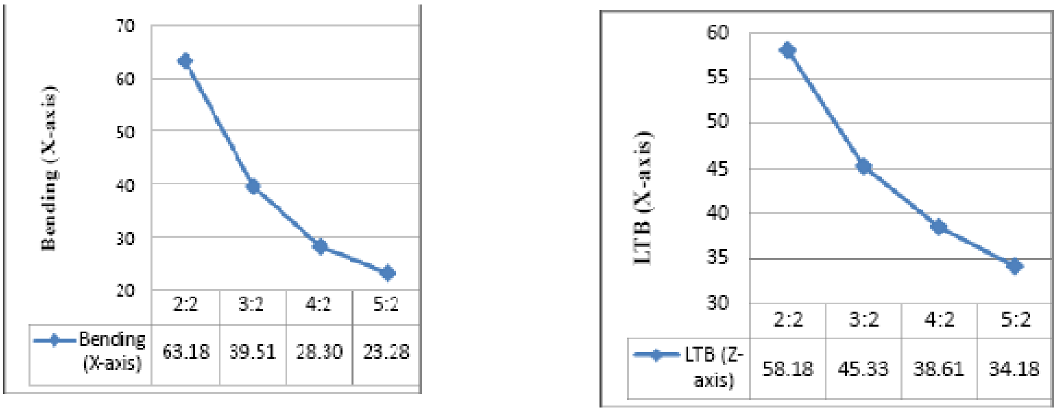


**Figure 2.2:** Effect of taper on bending and lateral torsional buckling [4]

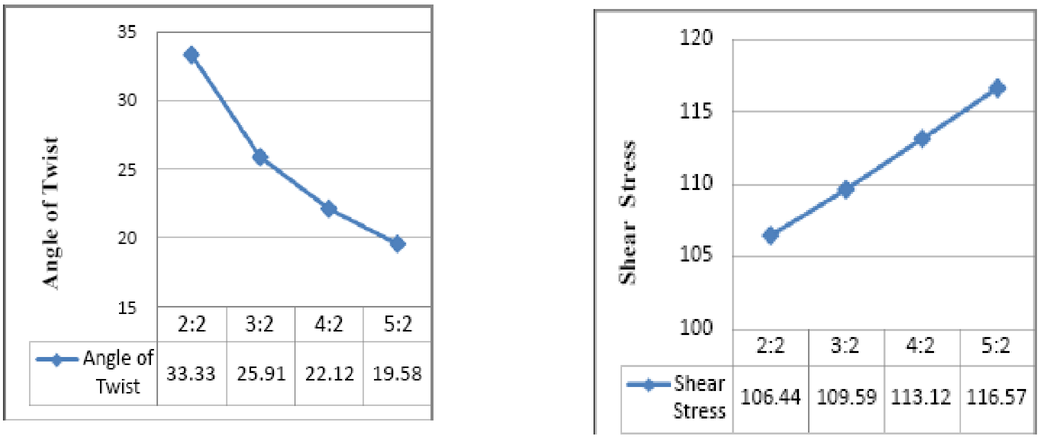


**Figure 2.3:** Effect of taper on angle of twist and Shear Stress [4]

From the results it was found that tapered steel beams are more resistant to bending and lateral torsional buckling than beams with flat webs. Also, with an increase in the taper ratio, angle of twist decreases and shear stress increases. Both Bending and Shear stress first decrease as the taperations increases up to taper ratio of 3:2, after which they decrease with an increase in the taper ratio. Hence consider taper ratio 3:2 as suitable ratio.

`

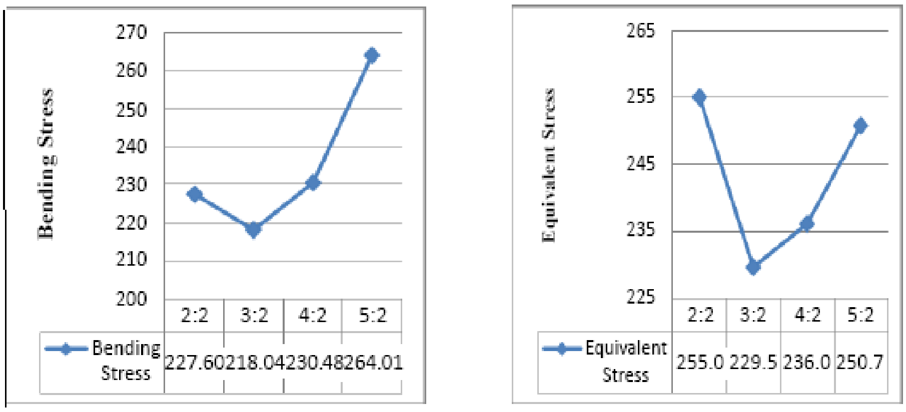


**Figure 2.4:** Effect of taper on Bending Stress and Equivalent Stress [4]

**Bending and torsion of hollow flange channel beams: Hong-Xia Wan and Mahen Mahendran [11].**

In this study the details of an investigation of the combination of bending and torsion behaviour of a hollow flange channel beam known as Lite Steel beam were presented using experiments and FEM. In the experimental study three LSB sections were tested to failure under a mid-span eccentric load. A special test rig was used to simulate different loading eccentricities and simple boundary conditions. Finite element models of tested LSBs were developed on ANSYS software, and their ultimate strengths, failure modes, load and displacement curves were obtained and further compared with corresponding test results. FEA and experimental results agreed well and thus validated the developed finite element models. The validated finite element models of LSB were used to conduct parametric studies to investigate the effects of the location and eccentricity of the applied load and change in spans. From the results it is seen that the bending moment capacity reduces considerably as the loading eccentricity increases.

**Shear stresses in tapered beams: Stefano Bennati, Paola Bertolini, Luca Taglialegne, and Paolo S.Valvo [3].**

In this paper the effects of taper on shear stresses in tapered beams were discussed. A symmetric tapered cantilever beam having length L, constant width b, and constant taper angle was considered which was made up of homogenous, linearly elastic homogenous material. The free end of the beam was loaded by an axial force N, shear force Q, moment M. The stress distribution in an elastic wedge loaded at the tip were determined in cartesian coordinates by using the exact solutions of Michel and Carothers and Galerkin and Knops as a starting point. Further the Strains and displacements were determined using

`

constitutive equations. The results were then compared to prismatic beam and it was found that when compared to prismatic beams, in tapered beams shear stresses were produced by shearing forces as well as by pure extension and bending. Also an expression for average shear stress was deduced at y = constant by imposing equilibrium of an infinitely small beam segment.

Further the exact and approximate solutions were compared by considering a different problem and it was found that it in case of shear stresses there was a good agreement between both the solutions. Also the results were validated through a finite element model of the similar problem on Abaqus software.

**Lateral Buckling Of Cold Formed Steel Beam with Trapezoidal Corrugated Web: R. Divahar and P. S. Joanna [15].**

In this study experimental study was performed on load carrying capacity of cold-formed steel section with trapezoid web. Six cold-formed steel beams with plain and trapezoidal webs were tested under two point loading for its pure flexural behaviour. After testing, the load carrying capacity of the steel beam with plain web and that of the beam with trapezoidal corrugated web having 300 and 450 corrugations were studied and compared. From the results, it can be seen that the load carrying capacity of the beam with trapezoidal web having 300 corrugations is higher than that of the beam having plain web as well as of the beam having 450 corrugations. Further it is seen that average load carrying capacity of cold-formed steel beams having 300 web corrugations increases by 25% of that of the beam with plain web. But there is only a slight increase between the load carrying capacity of the beam with 300 web corrugations and of the beam with 450 web corrugations. Also, in beams with plain web, shear buckling of web occurs, but this failure could be eliminated by using a corrugated web. In the beams with corrugated web strain is more than that of the beams with plain web.

**Lateral buckling of I-section composite beams: J. Lee, S.E. Kim, and K. Hong [29].**

In this study a one-dimensional finite element model was developed to study the lateral buckling of a composite I-section. The model developed is capable of predicting lateral buckling loads and moments for various configurations. The effects of different loading, difference in location of applied load and the fibre angle of web on buckling loads and moments of composite were studied. From the results it was concluded that orthotropic closed-form solution is not suitable for knowing about lateral buckling loads because of the presence of coupling stiffness for a beam under pure bending with off-axis fibre

`

orientation. It is also observed that when a transverse load is applied on a beam, the lateral buckling capacity is affected by fibre orientation. For all composite beams considered having all cases of span to height ratio, it is found that the maximum buckling load occurs at a fibre angle of 45$^{o}$ which means that the lateral buckling strength is dependent on torsional ridigity (*GJ*)com.

**Bending and buckling of tapered steel beam structures: Nicholas Trahair. [17]**

They analyzed the elastic in plane bending and out of plane buckling of indeterminate beam structures having tapered and mono symmetric I cross section members with the help of finite element method. A tapered mono symmetric structure was considered which is acted upon by a concentrated transverse and longitudinal load Q (at $y_Q$), N at($y_N$), and moment M along the axis Oz and distributed transverse and longitudinal loads q at $y_q$ and n at $y_n$ (Figure 2.5) The deformations were resisted by rigid or elastic restraints. Tapered finite element formulations were developed by numerical methods instead of closed forms which are used for uniform elements. For the tapered mono symmetric elements, the centroidal and the shear centre axes do not coincide, so the problem was simplified by using an arbitrary axis which lies on the web mid-line.

For the in plane bending analysis, a finite element method of analysis of a uniform beam column was considered, and necessary changes are made in that method corresponding to the arbitrary axis chosen for the mono symmetric tapered beam. A MATLAB computer program was written for this elastic in plane bending analysis. The program was further used for the analysis of tapered cantilevers and built in beams under various loading and restraint conditions. There is a very close agreement between the results of the program and the close form solutions of the beams.

For the flexural torsional buckling analysis, a finite element method of analyzing the flexural torsional buckling of a uniform member was considered, in which some changes to account for the inclination of the shear centre axis ,were made for the tapered members.

The MATLAB program for the elastic flexural torsional buckling of tapered beams was created based on this method and was used to analyze a number of mono symmetric uniform beams, doubly symmetric tapered beams, mono symmetric tapered beams and cantilevers. For the mono symmetric uniform cantilever beam and doubly symmetric tapered beam there is a close agreement between the program and theoretical results. For the mono symmetric tapered beams also, the results are in close agreement with theoretical

`

results. However, the results for the mono symmetric tapered cantilevers are a little less predictable than the others.

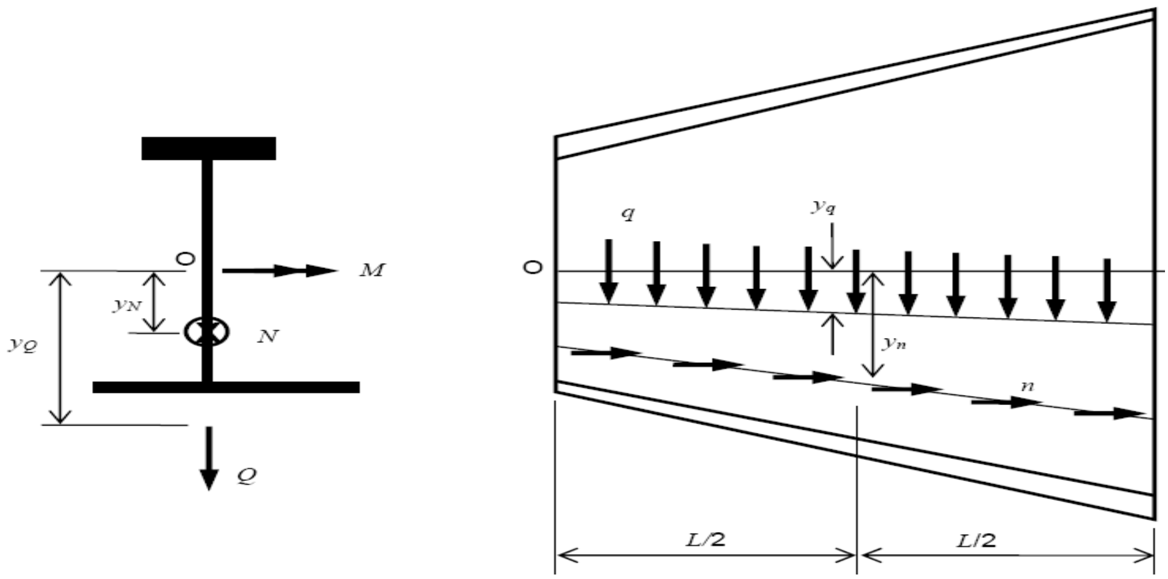


**Figure 2.5:** Mono symmetric tapered beams [17]

**Finite Element Analysis of Castellated Steel Beam: M.R. Wakchaure and A. V. Sagade [22]**

In this study, steel I beam was selected and castellated beams were fabricated with change in depth of web openings. To analyze the performance of castellated steel I beams modelling was done on FEM software ANSYS14. The beam is simply supported and acted upon by two point loads. Analysis is done and various failure patterns and deflection at the centre are studied. The beams with different depth of web openings were then compared to each other. From the finite element analysis results, it can be seen that, the castellated steel beam behaves reasonably up to a maximum web opening depth of 0.6h. Since castellated beams have holes in their web, it causes local failure modes in the beams which reduce their load carrying capacity. Hence, it is not feasible to compare the structural behaviour of beams having different modes of failure, based only on strength criteria. From the results, it is observed that as the depth of opening increases, stress concentrations, at the corners of the holes and at point of load application increases, and the flexural stiffness of castellated beams decreases. Therefore the serviceability performance of castellated beams can be improved in practice by applying various corrective measures, i.e. by making the hole corners round, by providing reinforcement at critical section, providing a plate below point

`

of application of the point load, etc. It is concluded that the castellated beams can be used well for industrial buildings, power plant and multi-storeyed buildings, with small loads and large spans

**Finite element stability analysis of tapered Beam-Columns: Vaidotas Sapalas, Michail Samofalov and Viaceslavas Saraskinas [28].**

In this paper theoretical and numerical analysis of tapered beam columns subjected to bending moment and an axial force were discussed. Further it was shown that the critical force of an axially loaded tapered column and the critical bending moment of a tapered column subjected to pure bending can be calculated by considering the column to be uniform with a correction factor $\alpha_{n,}$, $\alpha_m$ respectively. This correction factor is also called as the load multiplier and was calculated by a standard FEM code COSMOS/M.

In the theoretical analysis separate cases of a tapered column subjected to axial compression and bending moment were considered. For an axially loaded column the differential equation of a uniform column was first established and from that the critical force $N_{cr}$ was calculated. This force was then multiplied by the correction factor $\alpha_n$ to give critical force for the tapered column. For the pure bending case the value of critical bending moment was calculated by using the value of $M_{cr}$ from the European design code for a uniform beam with an I section. This value was then multiplied by the correction factor $\alpha_m$ to give the critical bending moment for the tapered column.

For the numerical analysis, FEM was used, where the column was simulated by using 2 kinds of finite elements, 1D for the column as a bar and 2D shell elements. The stability problem was analyzed by applying the 2D finite elements.

For the numerical solution of the axially loaded column and for a column subjected to pure bending, a large number of models were made within a wide range of second cross sectional moment of area of the column end 2 (Figure2.6) and from these simulations, correction factors $\alpha_{n,}$, $\alpha_m$ were obtained which when multiplied with the $N_{cr}$ and $M_{cr}$ of the uniform column, the critical force and bending moment for the tapered column was determined. From the results it is evident that these factors $\alpha_{n,}$, $\alpha_m$ depend on the ratio of end cross sectional moments of inertia $I_{y1}/I_{y2.}$ So these factors can be used for all types of column supports. Further it was suggested to use equivalent heights $h_{tr,n}$ ,$h_{tr,m}$ for practical calculations where $h_{tr,n} = \alpha_n .h2$ ,$h_{tr,m} = \alpha.$

`

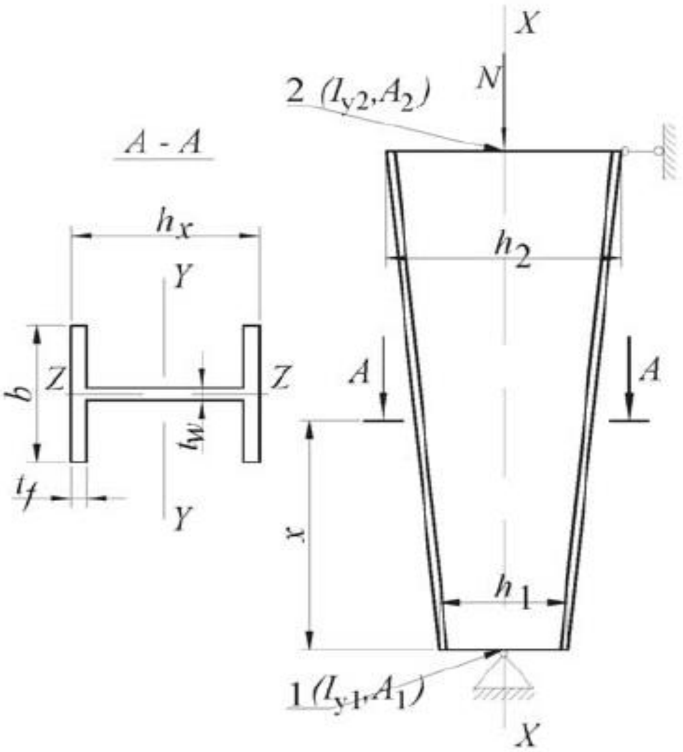


**Figure 2.6:** Axially loaded tapered column and its cross section [28]

**Lateral Torsional buckling of Non Prismatic I Beams: Gupta Pratyoosh, Wang S. T. and Blandford G.E [30].**

In this study a finite element program was developed to analyze the lateral torsional buckling of continuous, tapered I beams. This program was used to analyze beams with linear as well as quadratic taper for different support conditions (simply supported and fixed). The program predicted the buckling loads for web depth taper, flange width taper as well as flange thickness taper for continuous I beams where it has been observed that the maximum buckling load is achieved for flange thickness or flange width taper, and that the load increases gradually when the web depth is tapered. A study on the effect of increase in number of spans on buckling loads of non prismatic beams was also done where results show that the there is an increase in the buckling load from a single to double span beam, but beyond 2 spans, the change in the bucking capacity is very little.

After Literature Survey following Research objectives have been formulated.

`

## 2.2 Research Objectives

1) To study and analyze the lateral torsional buckling behavior of I beam of Jib Crane for self weight and vertical load at free end.
2) To study and analyze the effect of trapezoidal web on the lateral torsional buckling behaviour of the I beam of Jib Crane.
3) Comparison between the conventional I beam and the trapezoidal I beam for the buckling capacity and weight.

`

# CHAPTER 3

# METHODOLOGY

## 3.1 Finite Element Analysis

### 3.1.1 Objective

The objective of conducting finite element analysis is to predict the lateral torsional buckling behavior of I -section beam of a jib crane subjected to self weight and lifted load at the free end. A new design approach of using trapezoidal web corrugations in place of flat web of beam of the jib crane is proposed to predict the buckling behaviour of the beam and to check the economy and compare it with the flat web I beam. For the analysis purpose 32 3-D models of I - section beam with corrugated web are generated in AutoCAD and analysis is carried out in ANSYS Workbench 15.0. Further effect of web corrugations parameters and on buckling capacity, stress, is to be studied.

### 3.1.2 Overview of Finite Element Analysis

It is a numeric tool to get approximate solution of physical system. The design is modeled using discrete building blocks called elements. Each element has exact equations that describe how it responds to a certain load. The "sum" of the response of all elements in the model gives the total response of the design. The elements have finite number of unknowns, hence the name finite elements.

FEA has become a solution to the task of predicting failure due to unknown stresses by showing problem areas in a material and allowing designers to see all of the theoretical stresses within. This method of product design and testing is far superior to the manufacturing costs which would occur if each sample was actually built and tested. In practice, a finite element analysis usually consists of three principal steps,

**1. Pre-processing**

The user constructs a model of the part to be analyzed in which the geometry is divided into a number of discrete sub regions, or elements," connected at discrete points called nodes." Certain of these nodes will have fixed displacements, and others will have prescribed loads. These models can be extremely time consuming to prepare. Some of these pre-processors can overlay a mesh on a pre-existing CAD file, so that finite element analysis can be done conveniently as part of the computerized drafting-and-design process

`

**2. Solving**

The dataset prepared by the pre-processor is used as input to the finite element code itself, which constructs and solves a system of linear or nonlinear algebraic equations, where u and f are the displacements and externally applied forces at the nodal points. The formation of the K matrix is dependent on the type of problem being attacked, and this module will outline the approach for truss and linear elastic stress analyses. Commercial codes may have very large element libraries, with elements appropriate to a wide range of problem types.

**3. Post-processing**

In the earlier days of finite element analysis, the user would pore through reams of numbers generated by the code, listing displacements and stresses at discrete positions within the model. It is easy to miss important trends and hot spots this way, and modern codes use graphical displays to assist in visualizing the results.

Typical postprocessor display overlays colored contours representing stress levels on the model, showing a full field picture similar to that of photo elastic or mere experimental results.

### 3.1.3 Advantages of Finite Element Analysis

1. To reduce the amount of prototype testing.
2. Computer simulation allows multiple “what-if” scenarios to be tested quickly and effectively.
3. To simulate those designs which are not suitable for prototype testing.
4. Savings in Cost
5. Time savings

## 3.2 Methodology Adopted

Solving any problem on FEM software is like solving any problem analytically, we need to define (1) our solution domain, (2) the physical model, (3) boundary conditions and (4) the physical properties. Then solve the problem and obtain the results. In numerical methods, the main difference is an extra step called mesh generation. This is the step that divides the complex model into small elements that become solvable in an otherwise too complex situation. Solving any problem on FEM software involves following steps:

`

### 3.2.1 Creating Geometry

Geometry is created or a CAD file is imported into the software

### 3.2.2 Define material properties

Now that the part exists, define a library of the necessary materials that compose the object being modeled. This includes the mechanical properties as shown in Table 3.1.

**Table 3.1:** Material Properties

| Properties | Value |
|---|---|
| Density | 7850 ( $kg/m^3$) |
| Poisson's ratio | 0.3 |
| Young's modulus | $2.1\times10^5$ (MPa) |
| Tensile Ultimate Strength | 460 (MPa) |
| Tensile Yield strength | 250 (MPa) |

### 3.2.3 Generate Mesh

Mesh tool provides a number of options to mesh the object. The mesh can be 2D or 3D depending upon the requirement of the user. Given areas or volumes can be selected and meshed by proper selection.

### 3.2.4 Apply Loads

Once the system is fully designed, the last task is to burden the system with constraints, such as physical loadings and boundary conditions.

### 3.2.5 Obtain Solution

This is actually a step, because ANSYS needs to understand within what state (steady state, transient etc.) the problem must be solved.

### 3.2.6 Obtain the Results

After the solution has been obtained, there are many ways to present ANSYS results, which can be chosen from many options such as tables, graphs, and contour plots.

`

## 3.3 Work Plan

### 3.3.1 Selection of a Crane

Gorbel Crane FS-350 (Insert Mounted) is selected with the following crane parameters [35]:

- Capacity: 500 kg
- Rotation: 360°
- Span of Boom: 2.54 m
- Mast diameter 300 mm

Boom Dimensions: From ASTM A6, I beam S10@25.4lb/feet is selected with following section parameters [32] shown in Table 3.2.

**Table 3.2:** Beam Properties

| Designation | Depth (mm) | Width of flange (mm) | Thickness of web (mm) | Flange thickness (mm) |
|---|---|---|---|---|
| S10×25.4 | 254 | 12.5 | 8 | 118 |

### 3.3.2 Load Calculations:

Loads acting on the crane beam are calculated as follows [5]:

1. Trolley weight: the weight of the trolley and equipment attached to the trolley.
2. Dead load: the self weight of the beam and trolley.
3. Hoist load: The working load and the weight of the lifting devices.
4. Vertical Inertia Forces: Dead Load Factor + Hoist Load Factor. According to CMAA [31], Dead load factor equals to 1.2 and Hoist load factor equals to 0.15.
5. Inertia Forces from drive: The inertia forces occur during acceleration or deceleration or crane motions and depend on the driving and braking torques. Inertia forces from drives equals to 2.5% of the vertical load.

Load Calculation is shown in Table 3.3. For calculation of load, trolley position is assumed to be at the free end of the beam.

`

**Table 3.3:** Load Calculations

| | |
|---|---|
| 1. Lifted Load<br>Due to Impact load factor<br>Due to Dead load factor<br>Total | = 500 x 9.81= 4905N<br>= 0.25x4905 = 1226.25N<br>= 0.5 x 4905 = 2452.5 N<br>=8583.75 N<br>=8.58 KN |
| 2. Trolley Load<br>Due to Dead load | 149.68 x 9.81 =1.46 KN<br>1.2 x 1.46 = 1.752 KN |
| 3. Total Vertical Load= Lifted load + Trolley load | 8.58 + 1.46 + 1.752<br>= 11.792 KN |
| 4. Inertia forces from drive = 2.5% of Vertical Load | 2.5 x 11.792/100<br>= 0.2948 KN |
| 5. Total Test Load | =11.792 + 0.248<br>=12.04 KN or 12040 N |

### 3.3.3 I - Section Beam Analysis

Conventional beam of the crane will be first analyzed. For that the modeling is done on AutoCAD and analysis performed on ANSYS, procedure of which is explained later in this section. Further beams with trapezoidal corrugations in the web have to be developed in order to study and analyze the buckling behaviour of the beams. Figure 3.1 shows the top view of the proposed beam. For this purpose a total of 32 models with the following parameters are prepared and analyzed.

**Parameter selection:**

For trapezoidal web following parameters are selected:

i. Web thickness (tcw) – 6, 8 mm

ii. Corrugation angle (θ) – 30°, 45°, 60°, 75°

iii. Infill corrugation plate length (b) – 150, 250 mm

iv. Corrugation web width (h) – 25, 35 mm

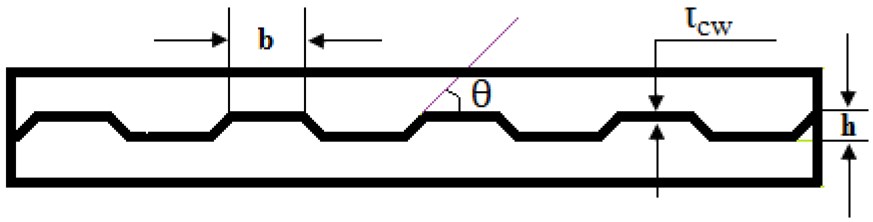


**Figure 3.1:** Top View of web

**Modeling**

AUTOCAD is used to create the models. First a conventional I beam with a plane web is modeled on AutoCAD as shown in Figure 3.2(a). Further 32 models with trapezoidal corrugated web are prepared with following parameters shown in Table 3.4.

**Table 3.4: Parameters of corrugated web section of various proposed beams**

| Sr. No | Web Thickness (mm) | Corrugation Plate Length (mm) | Corrugation Angles (Degree) | Corrugation Width (mm) |
|---|---|---|---|---|
| Model 1 | 6 | 150 | $30^o$ | 25 |
| Model 2 | 8 | 150 | $30^o$ | 25 |
| Model 3 | 6 | 150 | $45^o$ | 25 |
| Model 4 | 8 | 150 | $45^o$ | 25 |
| Model 5 | 6 | 150 | $60^o$ | 25 |
| Model 6 | 8 | 150 | $60^o$ | 25 |
| Model 7 | 6 | 150 | $75^o$ | 25 |
| Model 8 | 8 | 150 | $75^o$ | 25 |
| Model 9 | 6 | 150 | $30^o$ | 35 |
| Model 10 | 8 | 150 | $30^o$ | 35 |
| Model 11 | 6 | 150 | $45^o$ | 35 |
| Model 12 | 8 | 150 | $45^o$ | 35 |
| Model 13 | 6 | 150 | $60^o$ | 35 |
| Model 14 | 8 | 150 | $60^o$ | 35 |
| Model 15 | 6 | 150 | $75^o$ | 35 |
| Model 16 | 8 | 150 | $75^o$ | 35 |
| Model 17 | 6 | 250 | $30^o$ | 25 |
| Model 18 | 8 | 250 | $30^o$ | 25 |

`

| | | | | |
|---|---|---|---|---|
| Model 19 | 6 | 250 | 45° | 25 |
| Model 20 | 8 | 250 | 45° | 25 |
| Model 21 | 6 | 250 | 60° | 25 |
| Model 22 | 8 | 250 | 60° | 25 |
| Model 23 | 6 | 250 | 75° | 25 |
| Model 24 | 8 | 250 | 75° | 25 |
| Model 25 | 6 | 250 | 30° | 35 |
| Model 26 | 8 | 250 | 30° | 35 |
| Model 27 | 6 | 250 | 45° | 35 |
| Model 28 | 8 | 250 | 45° | 35 |
| Model 29 | 6 | 250 | 60° | 35 |
| Model 30 | 8 | 250 | 60° | 35 |
| Model 31 | 6 | 250 | 75° | 35 |
| Model 32 | 8 | 250 | 75° | 35 |

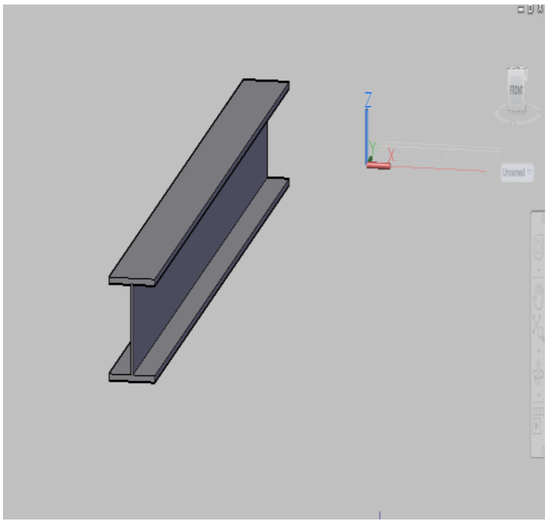

**Figure 3.2 (a):** Conventional I beam with a plane web

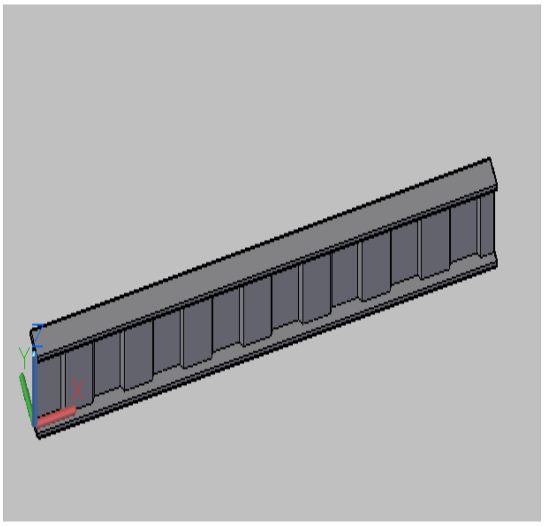

**Figure 3.2 (b):** I beam with trapezoidal corrugations in web

Analysis on ANSYS: For analysis ANSYS software is used. The procedure of the analysis is explained below. The same procedure is followed for flat as well as corrugated beam:

STEP 1: Engineering Data

First step of the analysis involves feeding the engineering data into the software ANSYS as shown in Figure 3.3.

STEP 2: Creating the Geometry

For creating geometry models are imported from AutoCAD on ANSYS as shown in Figure 3.4.

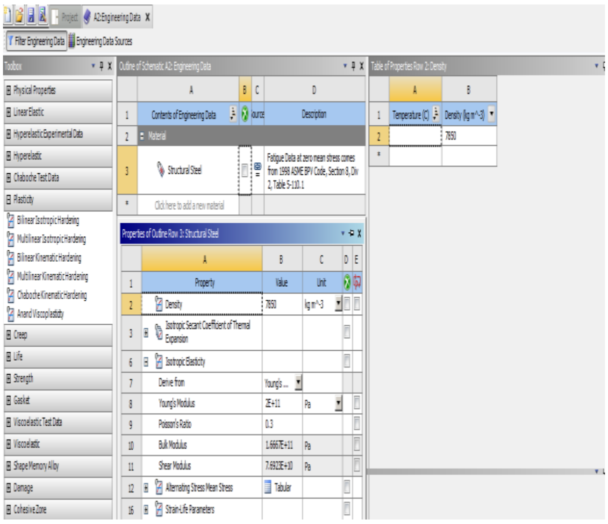

**Figure 3.3:** Engineering data fed into ANSYS

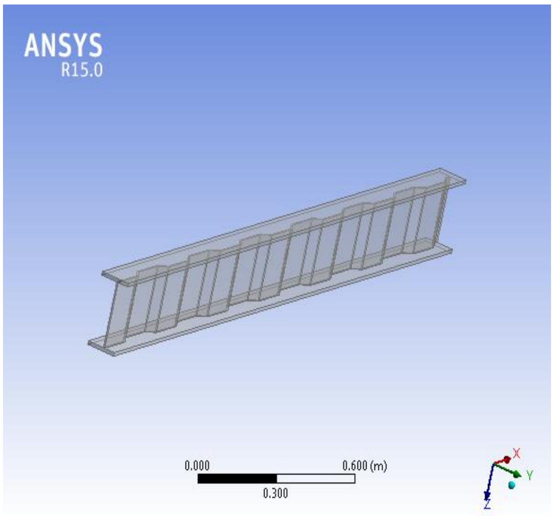


**Figure 3.4:** Geometry imported in ANSYS

STEP 3: Generate Mesh

Mesh tool provides a number of options to mesh the object. The mesh can be 2D or 3D depending upon the requirement of the user. Given areas or volumes can be selected and meshed by proper selection. To determine the size of the element a convergence study was conducted. Table 3.5 shows the data obtained after conducting the convergence study. From Figure 3.5 it can be seen that convergence is obtained at an element size of 10 mm. Therefore element size of 10mm is used in the analysis.

Figure 3.6 shows the mesh details in ANSYS.

`

**Table 3.5:** Data obtained from convergence study

| Mesh Size (mm) | Number of elements | Maximum Displacement(mm) |
|---|---|---|
| 70 | 5598 | 7.5194 |
| 60 | 5793 | 7.5176 |
| 50 | 7406 | 7.4189 |
| 40 | 7763 | 7.5174 |
| 30 | 13509 | 7.5077 |
| 20 | 17015 | 7.4632 |
| 10 | 30536 | 7.6598 |
| 5 | 121776 | 7.6599 |

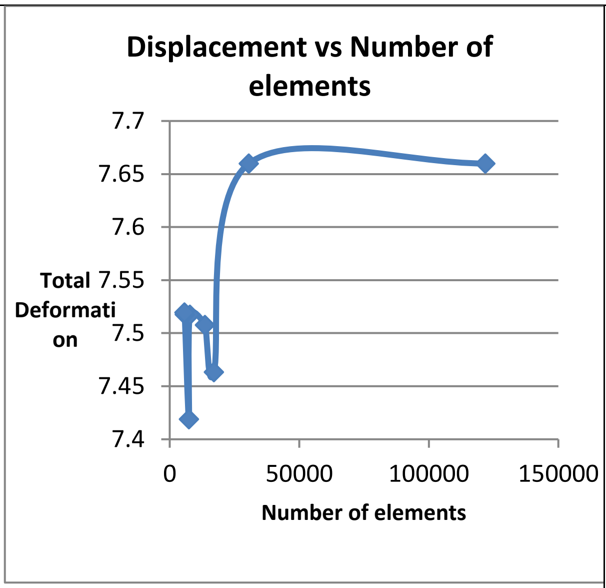


**Figure 3.5:** Convergence study graph

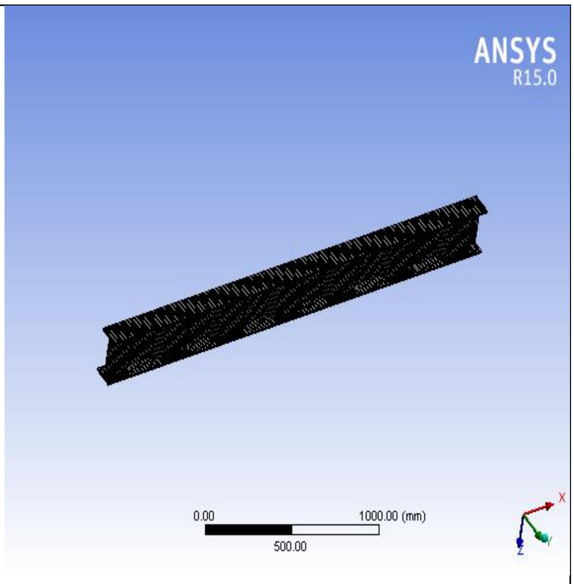


**Figure 3.6:**Mesh Details

STEP 4: Boundary Conditions and Load Application

Once the system is fully designed, the last task is to burden the system with constraints, such as physical loadings and boundary conditions. For support conditions left end of the beam is fixed and every movement is restricted in X, Y, Z directions as shown in Figure 3.7.For purpose of load application, total lifted load of 12040 N is distributed in an area of 118 × 100 mm from the free end applied in transverse direction to avoid any stress concentration. Figure 3.8 shows the application of load in ANSYS software.

`

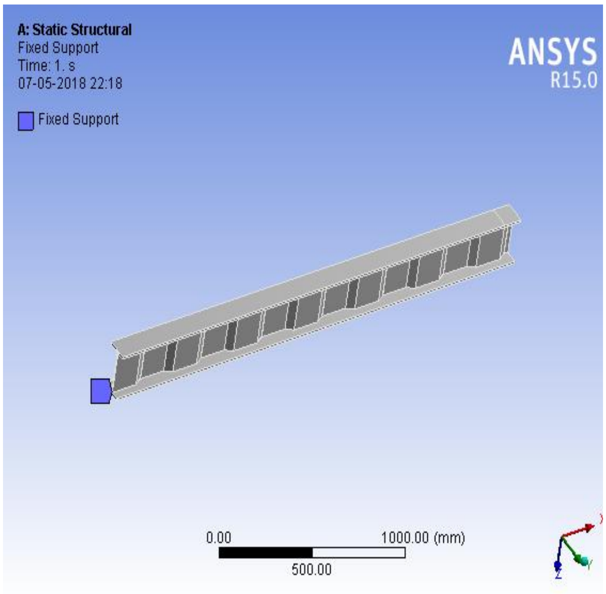


**Figure 3.7:** Fixed Support at the left end

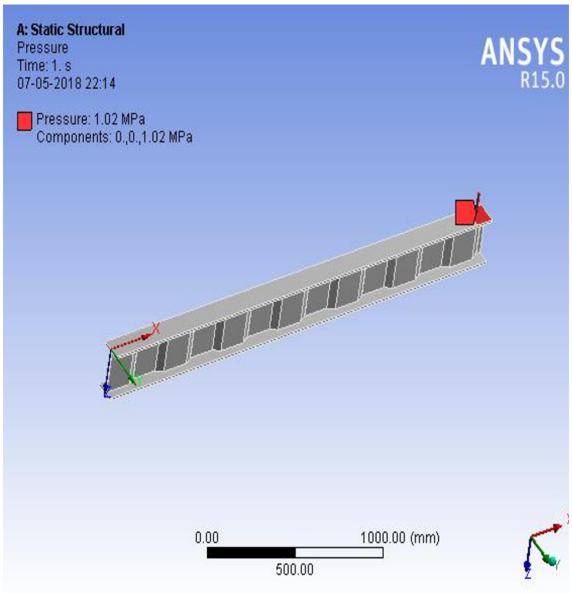


**Figure 3.8:** Load Application

STEP 5: Obtain Solution

After load application, the models are then analyzed for buckling load, Shear stress, Von Mises Stress and principal stress.

`

# CHAPTER 4

# RESULTS AND DISCUSSION

## 4.1 FEA RESULTS

### 4.1.1 FEA Results of a Flat Beam:

After Finite element analysis the results of buckling load, Maximum Shear Stress and Equivalent Stress have been tabulated in Table.4.1. Buckling load is calculated only for first mode by multiplying the load multiplier with the applied load.

**Table 4.1:** FEA results of a flat beam

| Buckling Load (KN) | Maximum Shear Stress (MPa) | Equivalent Stress (MPa) | Maximum Principal Stress (MPa) |
|---|---|---|---|
| 81.0 | 56.864 | 106.82 | 160.27 |

### 4.1.2 FEA Results of Corrugated Beams:

After Finite element analysis the results of buckling load, Maximum Shear Stress and Equivalent Stress have been tabulated in Table.4.2 - 4.5 to see the effects of corrugation web dimensions on structural capacities.

**Table 4.2:** FEA results of corrugated beam for Buckling load

<table>
<tr><th rowspan="2">Corrugation Plate Length</th><th rowspan="2">Web Width</th><th rowspan="2">Web Thickness</th><th colspan="4">Buckling load (KN)</th></tr>
<tr><th>$30^0$</th><th>$45^0$</th><th>$60^0$</th><th>$75^0$</th></tr>
<tr><td rowspan="4">150</td><td rowspan="2">25</td><td>6</td><td>71.32</td><td>84.73</td><td>86.48</td><td>87.84</td></tr>
<tr><td>8</td><td>88.25</td><td>90.24</td><td>92.00</td><td>93.82</td></tr>
<tr><td rowspan="2">35</td><td>6</td><td>85.44</td><td>87.71</td><td>94.48</td><td>94.76</td></tr>
<tr><td>8</td><td>91.01</td><td>93.34</td><td>95.95</td><td>99.39</td></tr>
<tr><td rowspan="4">250</td><td rowspan="2">25</td><td>6</td><td>70.22</td><td>83.22</td><td>83.00</td><td>83.83</td></tr>
<tr><td>8</td><td>86.57</td><td>88.81</td><td>89.80</td><td>89.85</td></tr>
<tr><td rowspan="2">35</td><td>6</td><td>84.15</td><td>84.00</td><td>87.49</td><td>87.56</td></tr>
<tr><td>8</td><td>89.28</td><td>90.05</td><td>93.45</td><td>93.731</td></tr>
</table>

`

**Table 4.3:** FEA results of corrugated beam for Maximum Shear Stress

| Corrugation Plate Length | Web Width | Web Thickness | Maximum Shear Stress (MPa) | | | |
|---|---|---|---|---|---|---|
| | | | **$30^0$** | **$45^0$** | **$60^0$** | **$75^0$** |
| 150 | 25 | 6 | 64.36 | 61.32 | 60.27 | 60.00 |
| | | 8 | 58.01 | 57.30 | 55.59 | 50.79 |
| | 35 | 6 | 61.31 | 60.93 | 55.34 | 53.00 |
| | | 8 | 56.32 | 55.79 | 54.54 | 49.14 |
| 250 | 25 | 6 | 64.64 | 62.31 | 60.99 | 60.64 |
| | | 8 | 58.07 | 57.33 | 56.143 | 55.82 |
| | 35 | 6 | 62.18 | 60.82 | 60.48 | 60.00 |
| | | 8 | 57.28 | 56.64 | 55.71 | 54.11 |

**Table 4.4:** FEA results of corrugated beam for Equivalent Stress

| Corrugation Plate Length | Web Width | Web Thickness | Equivalent Stress (MPa) | | | |
|---|---|---|---|---|---|---|
| | | | **$30^0$** | **$45^0$** | **$60^0$** | **$75^0$** |
| 150 | 25 | 6 | 118.5 | 113.39 | 111.10 | 110.93 |
| | | 8 | 109.24 | 107.81 | 108.25 | 108.00 |
| | 35 | 6 | 108.42 | 107.57 | 106.61 | 105.99 |
| | | 8 | 107.96 | 106.81 | 106.18 | 105.00 |
| 250 | 25 | 6 | 121.73 | 115.78 | 114.66 | 114.01 |
| | | 8 | 109.99 | 109.34 | 109.27 | 108.72 |
| | 35 | 6 | 116.96 | 115.32 | 114.00 | 113.28 |
| | | 8 | 110.32 | 109.08 | 108.35 | 107.23 |

`

**Table 4.5:** FEA results of corrugated beam for Maximum Principal Stress

| Corrugation Plate Length | Web Width | Web Thickness | Maximum Principal Stress (MPa) | | | |
|---|---|---|---|---|---|---|
| | | | $30^0$ | $45^0$ | $60^0$ | $75^0$ |
| 150 | 25 | 6 | 157.73 | 157.00 | 156.77 | 156.22` |
| | | 8 | 156.55 | 156.43 | 155.07 | 155.01 |
| | 35 | 6 | 156.91 | 156.12 | 155.00 | 155.96 |
| | | 8 | 156.42 | 156.00 | 154.20 | 154.82 |
| 250 | 25 | 6 | 158.06 | 157.93 | 157.91 | 156.99 |
| | | 8 | 157.43 | 156.63 | 156.11 | 156.00 |
| | 35 | 6 | 157.96 | 157.45 | 156.65 | 156.28 |
| | | 8 | 157.34 | 157.26 | 156.13 | 156.10 |

Further the results have been plotted in the form of graphs (Figure 4.1- 4.12) to see the effect of web corrugations on structure capacities.

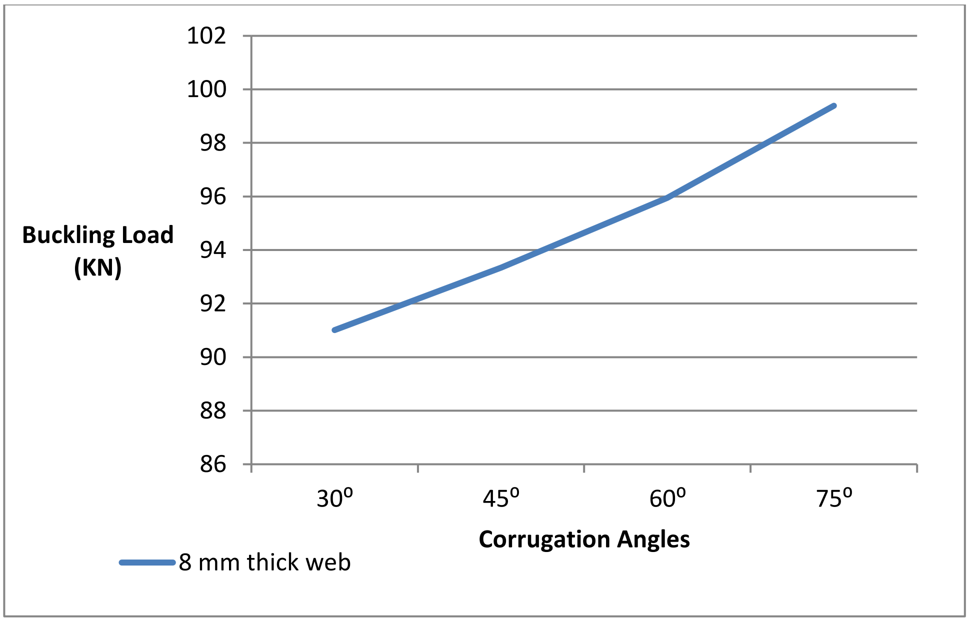


**Figure 4.1:** Effect of Corrugation Angles on Buckling Load

`

Figure 4.1 shows the effect of corrugation angles on buckling load for a beam having constant corrugation plate length of 150 mm, web width of 35 mm web thickness of 8mm. From Figure 4.1 it is seen that as the corrugation angles increase the buckling load also increases. Maximum buckling load occurs at $75^{o}$. From Table 4.1 it can be seen that the other beams also follow the same trend.

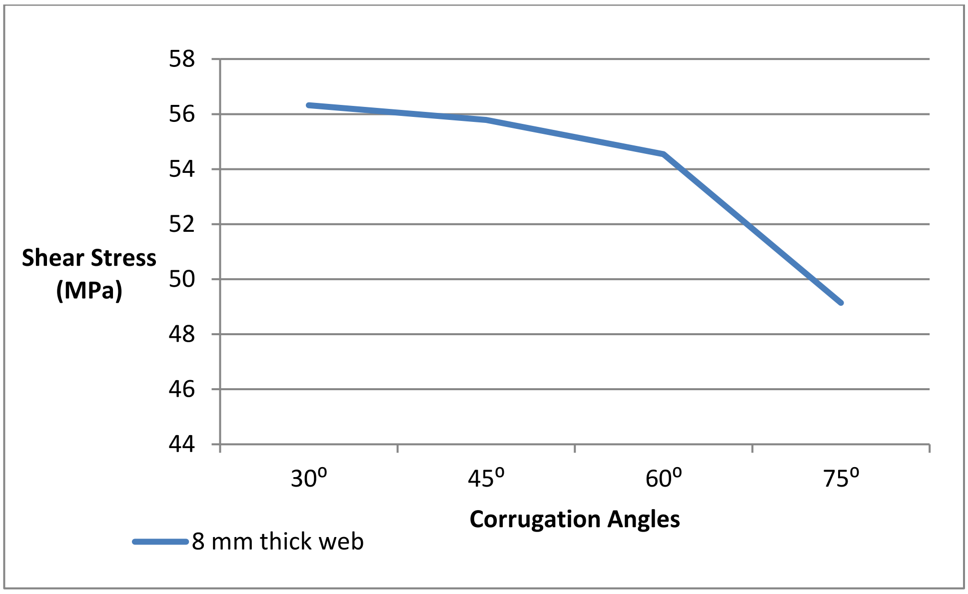


**Figure 4.2:** Effect of corrugation angle on Shear Stress

Figure 4.2 shows the effect of corrugation angle on shear stress for a beam having a constant web width of 35 mm, thickness 8 mm and corrugation plate length of 150mm .From Figure 4.2 it can be seen that for an increase in the corrugation angle, the shear stress decreases. When the angle is increased from $60^{o}$ to $75^{0}$ there is a sharp fall in stress. Minimum stress occurs at $75^{0}$. From Table 4.2 it can be seen that the same trend is followed by other beams as well.

Figure 4.3 shows effect of corrugation angles on equivalent stress for a beam having a constant web width of 35 mm, thickness 8 mm and corrugation plate length of 150 mm. From Figure 4.3 it can be seen that as the corrugation angle increases, the stress decreases but this change is very little. Minimum stress occurs at $75^{0}$. From Table 4.3 it is seen that the same trend is adopted by other beams as well.

`

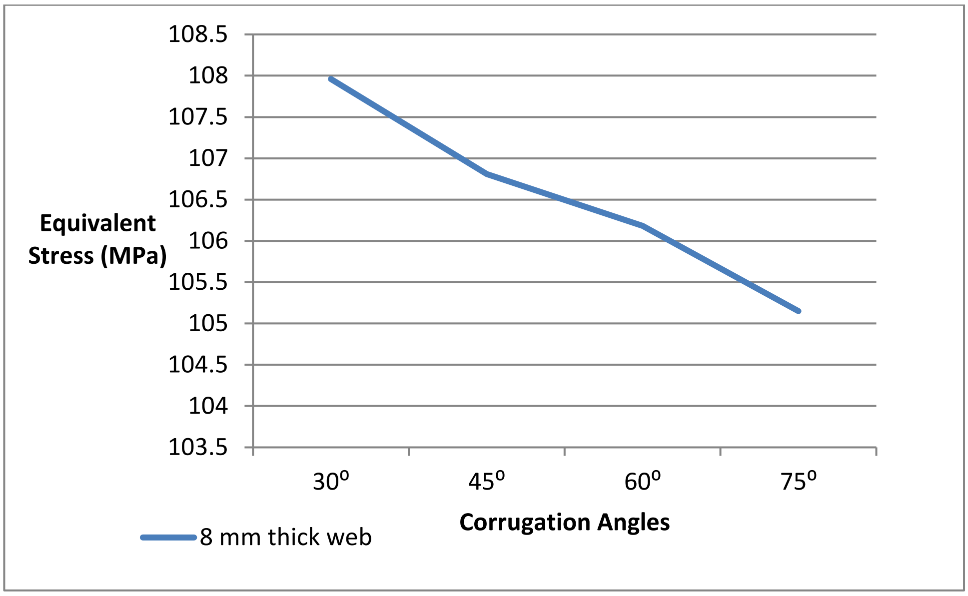


**Figure 4.3:** Effect of Corrugation angles on Equivalent Stress

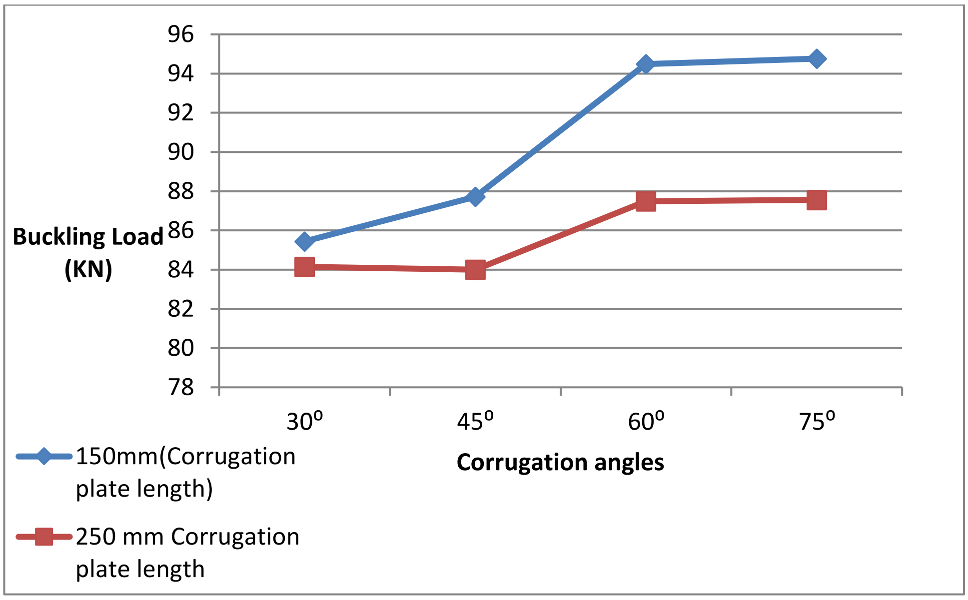


**Figure 4.4:** Effect of Corrugation plate length on Buckling Load

Figure 4.4 shows the effect of corrugation plate length on buckling load for a beam having constant web width of 35 mm, web thickness of 6 mm and variable corrugation plate length of 150 and 250 mm. From Figure 4.4 it can be seen as the corrugation plate length increases from 150mm to 250mm, there is a sharp fall in the buckling load for every corrugation angle. Maximum buckling load occurs at corrugation plate length of 150 mm having a corrugation angle $75^{0}$. From Table 4.1 it can be seen that other beams also follow the same trend.

`

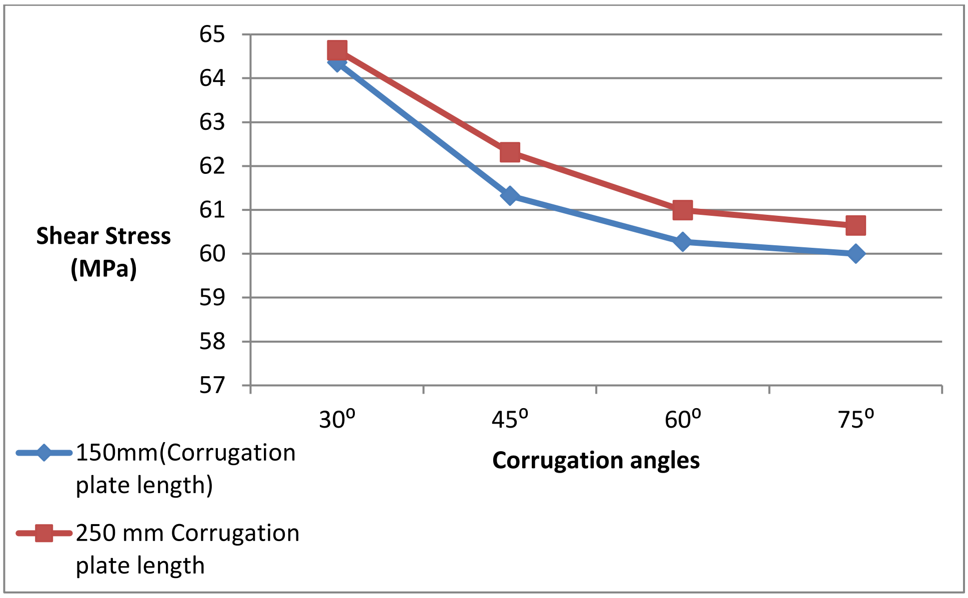


**Figure 4.5** Effect of Corrugation plate length on Shear Stress

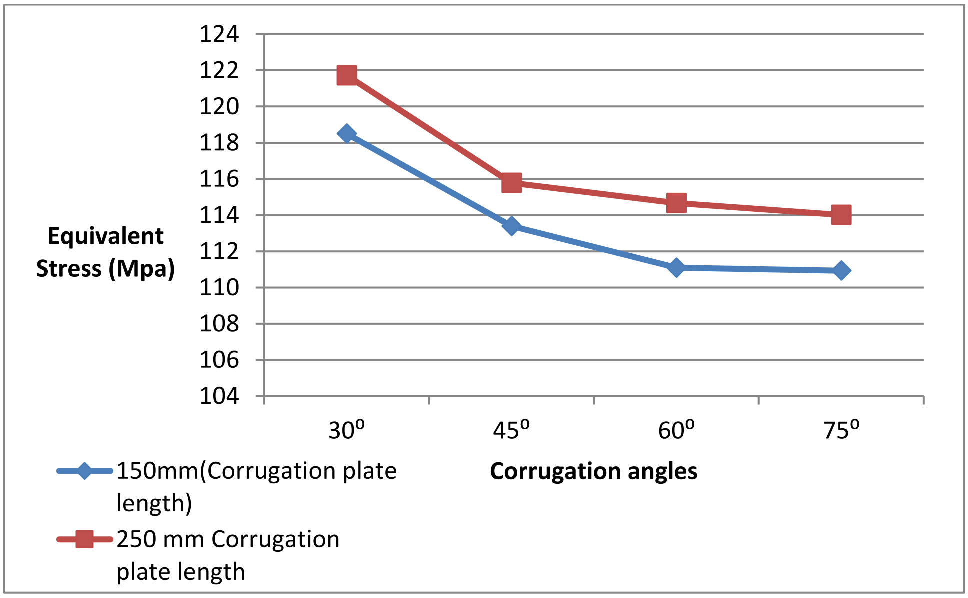


**Figure 4.6** Effect of Corrugation plate length on Equivalent Stress

Figure 4.5 shows the effect of corrugation plate length on shear Stress for a beam having a constant web width of 25 mm and thickness 6 mm and variable corrugation plate length of 150 and 250 mm respectively. From figure 4.5 it can be seen that as the plate length increases the shear stress increases and the minimum shear stress occurs for 150 mm plate length at $75^0$ corrugation angle. From Table 4.2 it can be seen that other beams also follow the same trend.

`

Figure 4.6 shows effect of Corrugation plate length on equivalent stress for a beam having a constant web width of 25 mm and thickness 6 mm and variable corrugation plate length of 150 and 250 mm respectively. From Figure 4.6 it can be seen that as the plate length increases the equivalent stress increases. The minimum stress occurs for 150 mm plate length and a 75$^{0}$ corrugation angle. From Table 4.3 it can be seen that other beams also follow the same trend.

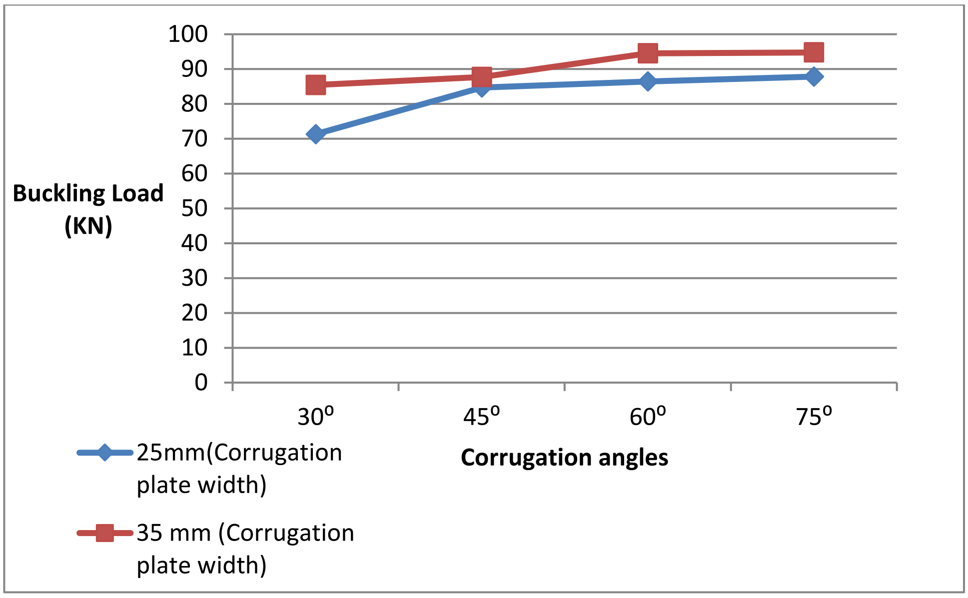


**Figure 4.7** Effect of Corrugation plate width on Buckling Load

Figure 4.7 shows the effect of corrugation plate width on buckling load for a beam having constant corrugation plate length of 150 mm and web thickness of 6 mm and variable web width of 25 and 35 mm respectively. From Figure 4.7 it can be seen that as the web width increases buckling load also increases and maximum buckling load occurs at 35 mm web width and corrugation angle of 75$^{0}$. From Table 4.1 it can be seen that the same trend is followed by other beams as well.

Figure 4.8 shows the effect of corrugation plate width on shear stress for a beam having constant corrugation plate length of 150 mm and web thickness of 6 mm and variable web width of 25 and 35 mm respectively. From Figure 4.8 it can be seen that as the web width increases shear stress decreases and minimum shear stress occurs at 35 mm web width and corrugation angle of 75$^{0}$. From Table 4.2 it can be seen that the same trend is followed by other beams as well.

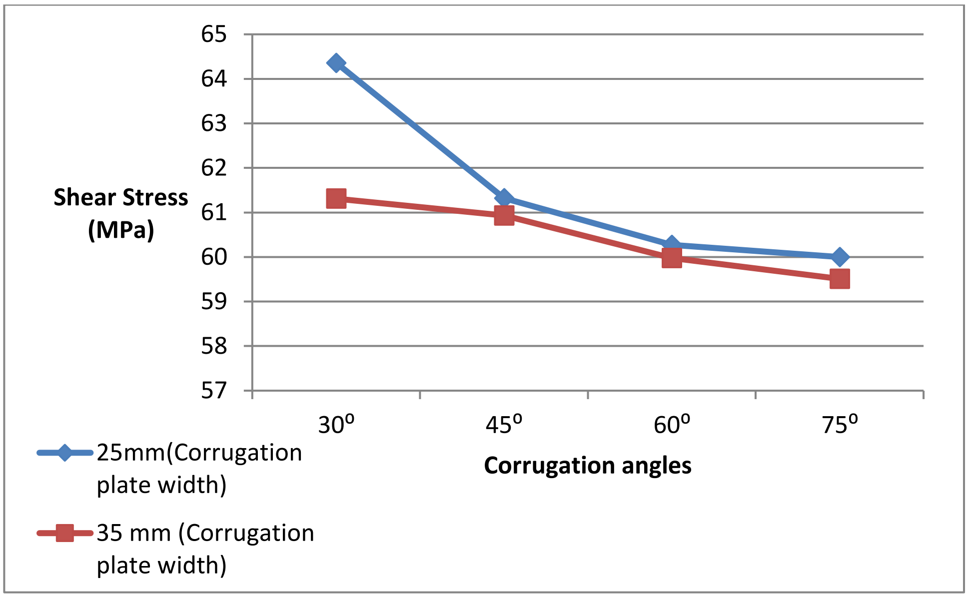


**Figure 4.8** Effect of Corrugation plate width on Shear Stress

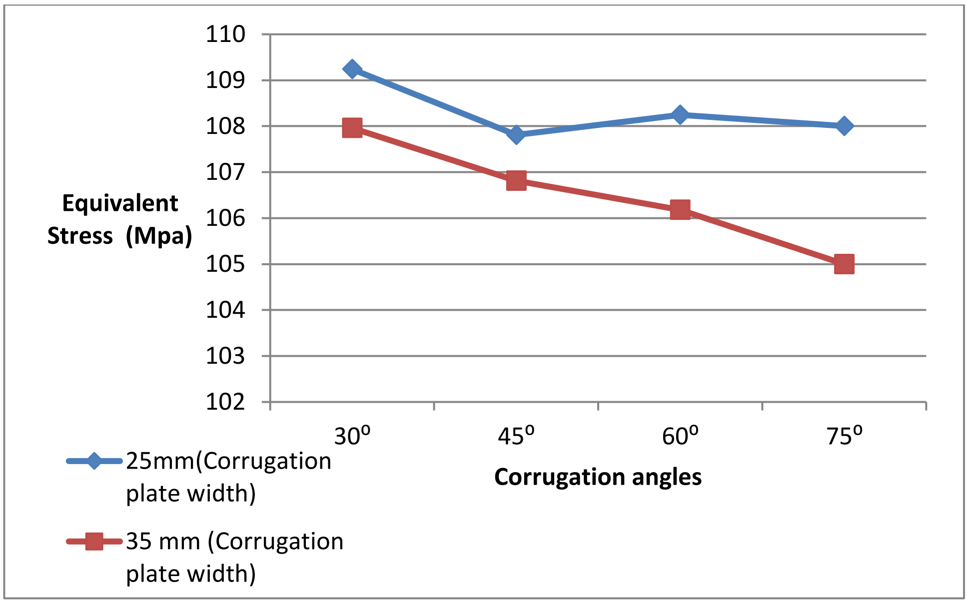


**Figure 4.9** Effect of Corrugation plate width on Equivalent Stress

Figure 4.9 shows the effect of corrugation plate width on equivalent stress for a beam having constant corrugation plate length of 150 mm and web thickness of 8 mm and variable web width of 25 and 35 mm respectively. From Figure 4.9 it can be seen that as the web width increases shear equivalnet decreases but this change is very little. Minimum shear stress occurs at 35 mm web width and corrugation angle of $75^0$. From Table 4.3 it can be seen that the same trend is followed by other beams as well.

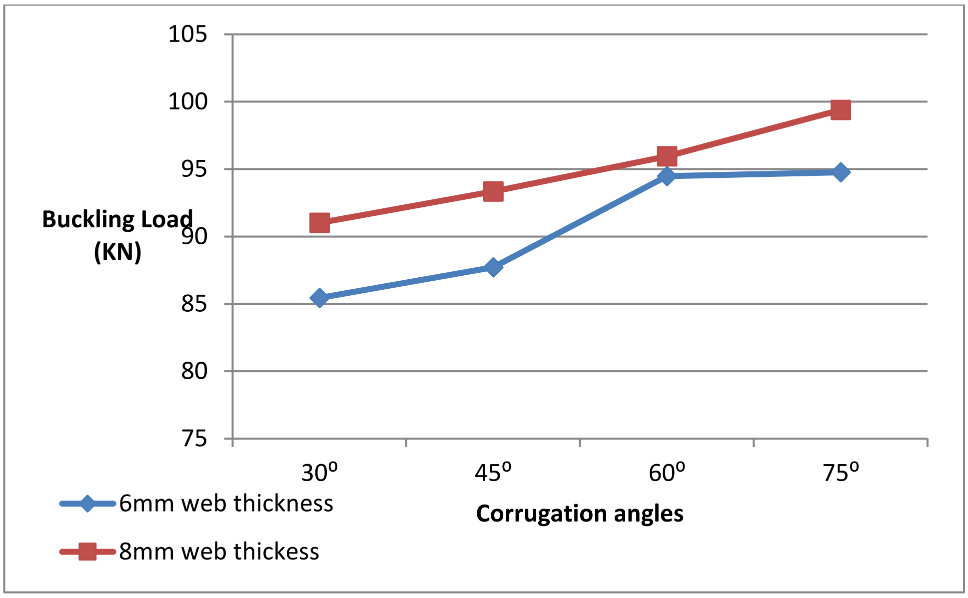


**Figure 4.10** Effect of Corrugation plate thickness on Buckling Load

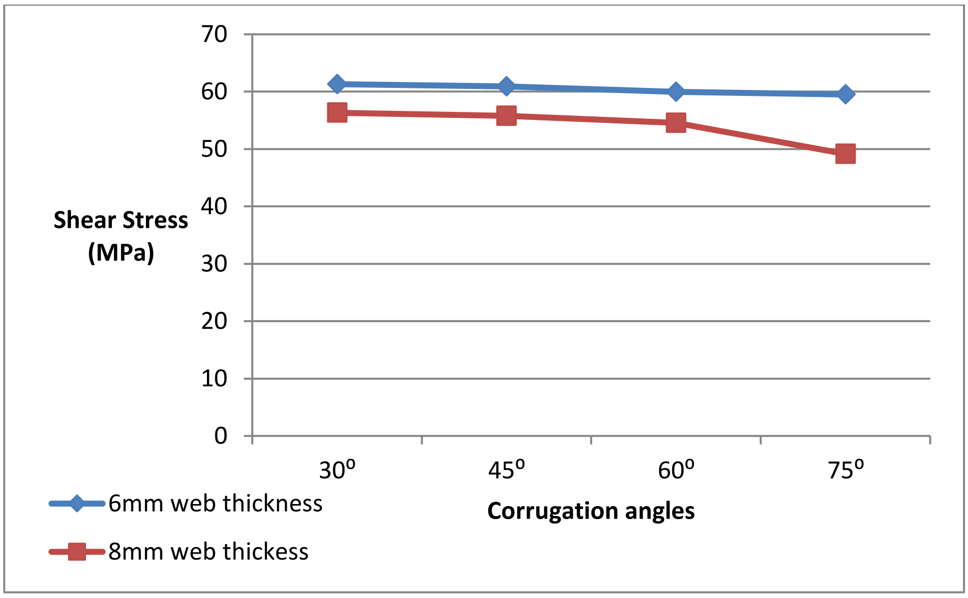


**Figure 4.11** Effect of Corrugation plate thickness on Shear Stress

Figure 4.10 shows the effect of corrugation plate thickness on buckling load for a beam having constant corrugation plate length of 150 mm and web width of 35 mm and variable web thickness of 6 and 8 mm respectively. From Figure 4.10 it can be seen that as the web thickness increases buckling load also increases. Maximum buckling load occurs at 8 mm web thickness and corrugation angle of $75^0$. From Table 4.1 it can be seen that the same trend is followed by other beams as well.

`

Figure 4.11 shows the effect of corrugation plate thickness on shear stress for a beam having constant corrugation plate length of 150 mm and web width of 35 mm and variable web thickness of 6 and 8 mm respectively. From Figure 4.11 it can be seen that as the web thickness increases shear stress decreases but this change is very little. Minimum shear stress occurs at 8 mm web thickness and corrugation angle of $75^0$. From Table 4.2 it can be seen that the same trend is followed by other beams as well.

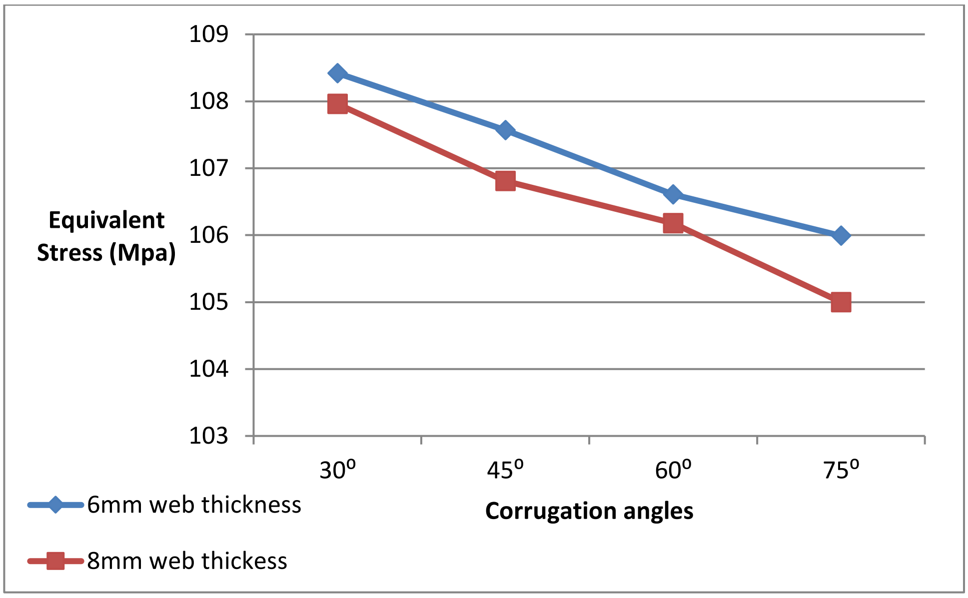


**Figure 4.12** Effect of Corrugation plate thickness on Equivalent Stress

Figure 4.12 shows the effect of corrugation plate thickness on equivalent stress for a beam having constant corrugation plate length of 150 mm and web width of 35 mm and variable web thickness of 6 and 8 mm respectively. From Figure 4.12 it can be seen that as the web thickness increases equivalent stress decreases but this change is very little. Minimum stress occurs at 8 mm web thickness and corrugation angle of $75^0$. From Table 4.2 it can be seen that the same trend is followed by other beams as well.

### 4.1.3 Comparison between Flat Beam and corrugated beam:

To choose the best model we have to first compare the flat beam with the 32 corrugated beams on the basis of weight and buckling load. The model which is to be chosen depends on two conditions.

**Condition 1:** The weight of the proposed beam should be less than that of the flat beam i.e. 95.348 kg.

**Condition 2:** The buckling load of the proposed beam should be greater than that of the flat beam i.e. 81 KN.

**Table 4.6:** Weight of the proposed corrugated beams.

| Corrugation Plate Length | Web Width | Web Thickness | Weight (kg) | | | |
|---|---|---|---|---|---|---|
| | | | $30^0$ | $45^0$ | $60^0$ | $75^0$ |
| 150 | 25 | 6 | 87.15 | 87.78 | 88.56 | 89.527 |
| | | 8 | 96.60 | 97.43 | 98.46 | 99.76 |
| | 35 | 6 | 74.93 | 88.24 | 89.32 | 90.56 |
| | | 8 | 96.96 | 98.05 | 99.48 | 101.17 |
| 250 | 25 | 6 | 86.79 | 87.225 | 87.61 | 88.07 |
| | | 8 | 96.11 | 96.69 | 97.21 | 97.21 |
| | 35 | 6 | 87.02 | 87.51 | 88.17 | 88.82 |
| | | 8 | 96.42 | 97.07 | 97.96 | 98.82 |

Table 4.6 shows the weight of the proposed corrugated beams extracted from the ANSYS software. From Table 4.1 and 4.6, based on above 2 conditions the corrugated beam is compared to the flat beam and the best model is chosen. Table 4.7 shows the results obtained after the comparison of the flat beam and corrugated beam.

**Table 4.7:** Comparative Results between the flat beam and corrugated beam

| Model | Weight (Kg) | Buckling Load(KN) | Maximum Shear Stress(MPa) | Equivalent Stress (MPa) | Maximum Principal Stress (MPa) |
|---|---|---|---|---|---|
| Flat Beam | 95.48 | 81.0 | 56.864 | 106.82 | 160.27 |
| Corrugated Beam | 89.32 | 94.48 | 55.34 | 106.61 | 155.00 |

After comparing the flat beam to the corrugated beam it can be seen model number 13 having a corrugation plate length of 150mm, web width of 35mm, web thickness of 6mm and corrugation angle $60^0$ offers higher buckling load and is more light and economical than the flat beam. Result files of both these models i.e. the flat beam and best optimized corrugated beam is shown in appendix.

`

# CHAPTER 5

# CONCLUSION

## 5.1 Conclusion

In this study a new design approach of using a web with trapezoidal corrugations for a beam of a jib crane is proposed, to study the lateral torsional buckling behaviour of the beam subjected to self weight and lifted load at free end. After conducting the finite element analysis of the flat beam of the jib crane and comparing with the proposed corrugated web beams, following points are concluded:

1. Steel I beam with trapezoidal corrugated web offers higher resistance to lateral torsional buckling as compared to the conventional steel I beam having a flat web.
2. Steel I beam with trapezoidal corrugated web produces less shear, equivalent and principal stresses than the conventional steel I beam with a flat web.
3. Model number 13 i.e. beam having a corrugation plate length of 150 mm, web width of 35 mm, web thickness of 6 mm and corrugation angle $60^0$ offers higher buckling load and is more light and economical than the flat beam.
4. Trapezoidal web thickness, corrugation angle, length of corrugated plate, width of corrugated web influences the resistance to lateral torsional buckling and shear stress in following ways:
    a. Higher trapezoidal web thickness results in higher resistance to lateral torsional buckling.
    b. Increasing the length of corrugated plate reduces the resistance to lateral torsional buckling.
    c. Increasing the width of corrugated web increases the resistance to lateral torsional buckling.
    d. Corrugation angle of $75^0$ results in higher resistance to lateral torsional buckling.

## 5.2 Scope for future work:

1 This work can be further extended to carry out an experimental setup for validation of the numerical analysis work.

2 This work can be further extended for the numerical analysis of composite sections.

`

# REFERENCES


[1] Dandavatimath, C.C. and Sarode, H.D. (2017). “Finite element analysis and Optimization of Jib Crane Boom”, *International journal of innovative research in Science, Engineering and Technology*, 6(7), 14287-14294.

[2] Fatima denan, Keong, C.K., and Hashim, N.S. (2017). “The effects of the depth of web on the bending behaviour of triangular web profile steel beam section”, *American Institute of Physics, AIP Conference Proceedings 1892,*020022, 1-8.

[3] Stefano, B., Bertolini, P., Taglialegne, L. and Valvo, P.S. (2016). “Conference Paper on Shear stresses in tapered beams”, *21st Italian Conference on Computational Mechanics, at Lucca,* 83-84.

[4] Patil, T. and Shelke, N.L. (2016). “Structural Analysis of a cantilever Beam with tapered web section through FEA”, *Journal of Steel Structures and Construction,* 2(2), 1-6.

[5] Dhanusha, M. and Reddy, V.G. (2016). “Detail Design and Analysis of A Free Standing I Beam Jib Crane’’, *International Research Journal of Engineering and Technology*, 3(12), 193-203.

[6] Amreeta, R.K. and Singh, V. (2015). “Design and stress analysis of single girder jib crane’’, *International Journal of Engineering Research and Technology,* 4(9), 932-936.

[7] Rajmane, S.M. and Jadhav, A. (2015). “Finite element analysis of jib crane’’, *International Journal of Innovative Research in Technology,* 2(6), 404-407.

[8] Chaudhary, A.S. and Khan, S.N. (2015).”Design and analysis of varying cross sectional cantilever beam with trapezoidal web for Jib crane”, *International Engineering Research Journal,* Special Issue 2, 4475-4480.

[9] Kapadni, K.R. and Ganiger, S.G. (2015). “Review paper on design and structural analysis of simply supported gantry crane beam for eccentric loading”, *International Research Journal of Engineering and Technology,* 2(8), 1622-1626.

[10] Kiranalli, S.S. and Patil, N.U. (2015). “Jib Crane Analysis using FEM”, *International Journal for Scientific Research and Development*, 3(4), 185-189.

[11] Wan, H.X. and Mahendran, M., (2015). “Bending and torsion of hollow flange channel beams” *Engineering Structures 84,* 300–312.

`


[12] Bollimpelli, K.S. and Kumar, V.R. (2015). "Design and Analysis of Column Mounted JIB Crane", *International Journal of Research in Aeronautical and Mechanical Engineering*, 3(1), 32-52.

[13] Arvind Kumar, V.C. (2015). "Design and Analysis of Beam for Deformation of Floor Mounted Jib Crane", *M.Tech. Thesis, Gujarat Technical University.*

[14] Khetre, N.S., Bankar, P.S. and Meshram, A.M. (2014). "Design and Static Analysis of I section Boom for Rotary Jib Crane", *International Journal of Engineering Research and Technology*, 3(8), 1071-1074.

[15] Divahar, R. and Joanna, P.S. (2014). "Lateral Buckling Of Cold Formed Steel Beam with Trapezoidal Corrugated Web", *International Journal Of Civil Engineering And Technology*, 5(3), 217-225.

[16] Ozbasaran, H. (2014). "A parametric study on lateral torsional buckling of European IPN and IPE cantilevers", *International Journal of Civil, Architectural, Structural and Construction Engineering*, 8(7), 783-788.

[17] Trahair, N. (2014). "Bending and Buckling Of Tapered Steel Beam Structures", *Engineering Structures 59*, Science Direct, Elsevier, 229–237.

[18] Fatimah De'nan, Mustar, M., Hassan, A.B. and Omar, N. (2013). "Effect of Triangular Web Profile on the Shear Behaviour of Steel I-Beam, *Iranica Journal of Energy & Environment,* 4 (3), 219-222.

[19] Suratkar, A., Shukla, V. and Zakiuddin, K.S. (2013). "Design Optimization of Overhead EOT Crane Box Girder Using Finite Element Analysis", *International Journal of Engineering Research & Technology*, 2(7), 720-724.

[20] Limaye, A. A. and Alandkar, P.M. (2013). "Strength of Welded Plate Girder with Corrugated Web Plate", *International Journal of Engineering Research and Applications*, 3(5), 1925-1930.

[21] Gerdemeli, I., Kurt, .S. and Tasdemir, B. (2012). "Design and Analysis with Finite Element Method of Jib Crane", *Mechanical Engineering Istanbul Technical University – Turkey*, 565-568.

[22] Wakchaure, M.R., Sagade, A.V. (2012). "Finite Element Analysis of Castellated Steel Beam", *International Journal of Engineering and Innovative Technology*, 2(1), 365-372.

`


[23] Fatimah De'nan and Hashim, N.S. (2011). "The effect of web corrugation angle on bending performance of triangular web profile steel beam section", *International Journal of Environmental Protection*, 1(5), 53-56.

[24] Fatimah De'nan, Osman, M.H. and Saad, S. (2010). "The Study of Lateral Torsional Buckling Behaviour of Beam With Trapezoid Web Steel Section By Experimental And Finite Element Analysis", *International Journal of Recent Research and Applied Studies,* 2 (3), 232-240.

[25] Gerdemeli, I., Kurt, S. and Alkan, H.O. (2010). "Main Girder Beam Design and Finite Element Analysis of 2x160 Ton Gantry Crane", *14th International Research/Expert Conference Trends in the Development of Machinery and Associated Technology, Mediterranean Cruise,* 565-568.

[26] Moon, J., Yi, J.W., Choi, B.H., Lee, H.E. (2009). "Lateral Torsional Buckling of I girder with corrugated webs under uniform bending", *Thin Walled structures,* Elsevier, 47(1), 21-30.

[27] Brettle, M. (2005). "Lateral Torsional Buckling and slenderness', Technical Paper, New Steel Construction, 30-34.

[28] Sapalas,V., Samofalov, M., Saraskinas, V. (2005). "Finite element stability analysis of tapered Beam-Columns", *Journal of Civil Engineering and Management,* 11(3), 211-216.

[29] Lee, J., Kim, S.E. and Hong, K. (2002). "Lateral buckling of I section composite beams", *Engineering Structures 24,* Science Direct, Elsevier, 955–964.

[30] Gupta, P., Wang, S.T. and Blandford, G.E. (1995). "Lateral Torsional buckling of Non Prismatic I Beams", *Journal of Structural Engineering,* 122(7), 748-755.

[31] Crane Manufacturers Association of America Specifications-74

[32] ASTM A6: Standard Specification for General Requirements for Rolled Structural Steel Bars, Plates, Shapes and Sheet Piling.

[33] ANSYS 14.0

[34] AutoCAD 2015

[35] Gorbel User Manual www.gorbel.com/authorizedusers.asp

`

# APPENDIX A

ANSYS report file of flat beam:

Project

| | |
|---|---|
| First Saved | Tuesday, December 12, 2017 |
| Last Saved | Saturday, May 05, 2018 |
| Product Version | 15.0 Release |
| Save Project Before Solution | No |
| Save Project After Solution | No |

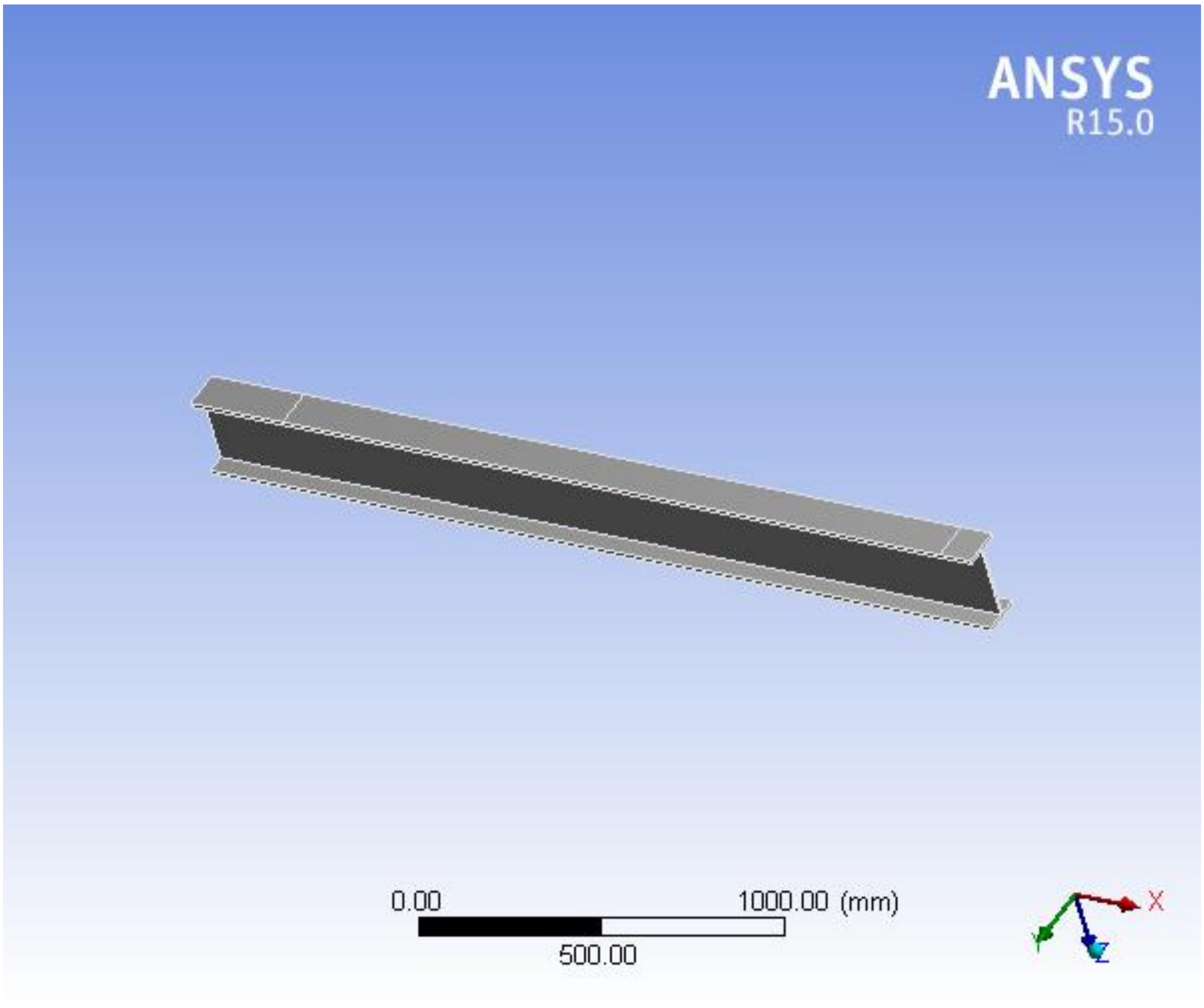

`

## Contents



## Units

**TABLE 1**

| | |
|---|---|
| Unit System | Metric (mm, kg, N, s, mV, mA) Degrees rad/s Celsius |
| Angle | Degrees |
| Rotational Velocity | rad/s |
| Temperature | Celsius |

## Model (A4, B4)

### Geometry

**TABLE 2**
**Model (A4, B4) > Geometry**

| | |
|---|---|
| Object Name | *Geometry* |
| State | Fully Defined |
| **Definition** | |
| Source | C:\Users\Inspiron\Desktop\damini files2\basic part analysis\fgffgfg_files\dp0\SYS\DM\SYS.agdb |
| Type | DesignModeler |

`

| | |
|---|---|
| Length Unit | Millimeters |
| Element Control | Program Controlled |
| Display Style | Body Color |
| **Bounding Box** | |
| Length X | 2540. mm |
| Length Y | 118. mm |
| Length Z | 254. mm |
| **Properties** | |
| Volume | 1.2146e+007 $mm^3$ |
| Mass | 95.348 kg |
| Scale Factor Value | 1. |
| **Statistics** | |
| Bodies | 1 |
| Active Bodies | 1 |
| Nodes | 54858 |
| Elements | 26665 |
| Mesh Metric | None |
| **Basic Geometry Options** | |
| Parameters | Yes |
| Parameter Key | DS |
| Attributes | No |
| Named Selections | No |
| Material Properties | No |
| **Advanced Geometry Options** | |
| Use Associativity | Yes |
| Coordinate Systems | No |
| Reader Mode Saves | No |

`

| | |
|---|---|
| Updated File | |
| Use Instances | Yes |
| Smart CAD Update | No |
| Compare Parts On Update | No |
| Attach File Via Temp File | Yes |
| Temporary Directory | C:\Users\Inspiron\AppData\Roaming\Ansys\v150 |
| Analysis Type | 3-D |
| Decompose Disjoint Geometry | Yes |
| Enclosure and Symmetry Processing | Yes |

**TABLE 3**
**Model (A4, B4) > Geometry > Parts**

| Object Name | *Solid* |
|---|---|
| State | Meshed |
| **Graphics Properties** | |
| Visible | Yes |
| Transparency | 1 |
| **Definition** | |
| Suppressed | No |
| Stiffness Behavior | Flexible |
| Coordinate System | Default Coordinate System |
| Reference Temperature | By Environment |
| **Material** | |
| Assignment | Structural Steel |
| Nonlinear Effects | Yes |
| Thermal Strain Effects | Yes |

`

| Bounding Box | |
|---|---|
| Length X | 2540. mm |
| Length Y | 118. mm |
| Length Z | 254. mm |
| **Properties** | |
| Volume | 1.2146e+007 mm³ |
| Mass | 95.348 kg |
| Centroid X | 1270. mm |
| Centroid Y | 2.1725e-014 mm |
| Centroid Z | 127. mm |
| Moment of Inertia Ip1 | 1.0865e+006 kg·mm² |
| Moment of Inertia Ip2 | 5.228e+007 kg·mm² |
| Moment of Inertia Ip3 | 5.1331e+007 kg·mm² |
| **Statistics** | |
| Nodes | 54858 |
| Elements | 26665 |
| Mesh Metric | None |

## Coordinate Systems

**TABLE 4**
**Model (A4, B4) > Coordinate Systems > Coordinate System**

| | |
|---|---|
| Object Name | *Global Coordinate System* |
| State | Fully Defined |
| **Definition** | |
| Type | Cartesian |
| Coordinate System ID | 0. |
| **Origin** | |
| Origin X | 0. mm |

`

| | |
|---|---|
| Origin Y | 0. mm |
| Origin Z | 0. mm |
| **Directional Vectors** | |
| X Axis Data | [1. 0. 0. ] |
| Y Axis Data | [0. 1. 0. ] |
| Z Axis Data | [0. 0. 1. ] |

## Mesh

**TABLE 5**
**Model (A4, B4) > Mesh**

| Object Name | Mesh |
|---|---|
| State | Solved |
| **Defaults** | |
| Physics Preference | Mechanical |
| Relevance | 0 |
| **Sizing** | |
| Use Advanced Size Function | Off |
| Relevance Center | Coarse |
| Element Size | 10.0 mm |
| Initial Size Seed | Active Assembly |
| Smoothing | Medium |
| Transition | Fast |
| Span Angle Center | Coarse |
| Minimum Edge Length | 12.50 mm |
| **Inflation** | |
| Use Automatic Inflation | None |
| Inflation Option | Smooth Transition |
| Transition Ratio | 0.272 |

`

| | |
|---|---|
| Maximum Layers | 5 |
| Growth Rate | 1.2 |
| Inflation Algorithm | Pre |
| View Advanced Options | No |
| **Patch Conforming Options** | |
| Triangle Surface Mesher | Program Controlled |
| **Patch Independent Options** | |
| Topology Checking | Yes |
| **Advanced** | |
| Number of CPUs for Parallel Part Meshing | Program Controlled |
| Shape Checking | Standard Mechanical |
| Element Midside Nodes | Program Controlled |
| Straight Sided Elements | No |
| Number of Retries | Default (4) |
| Extra Retries For Assembly | Yes |
| Rigid Body Behavior | Dimensionally Reduced |
| Mesh Morphing | Disabled |
| **Defeaturing** | |
| Pinch Tolerance | Please Define |
| Generate Pinch on Refresh | No |
| Automatic Mesh Based Defeaturing | On |
| Defeaturing Tolerance | Default |
| **Statistics** | |

`

| | |
|---|---|
| Nodes | 54858 |
| Elements | 26665 |
| Mesh Metric | None |

## Static Structural (A5)

**TABLE 6**
**Model (A4, B4) > Analysis**

| **Object Name** | ***Static Structural (A5)*** |
|---|---|
| **State** | **Solved** |
| **Definition** | |
| Physics Type | Structural |
| Analysis Type | Static Structural |
| Solver Target | Mechanical APDL |
| **Options** | |
| Environment Temperature | 22°C |
| Generate Input Only | No |

**TABLE 7**
**Model (A4, B4) > Static Structural (A5) > Analysis Settings**

| **Object Name** | ***Analysis Settings*** |
|---|---|
| State | Fully Defined |
| **Restart Analysis** | |
| Restart Type | Program Controlled |
| Status | Done |
| **Step Controls** | |
| Number Of Steps | 1. |
| Current Step Number | 1. |
| Step End Time | 1. s |
| Auto Time Stepping | Program Controlled |

`

| Solver Controls | |
|---|---|
| Solver Type | Program Controlled |
| Weak Springs | Program Controlled |
| Large Deflection | Off |
| Inertia Relief | Off |
| **Restart Controls** | |
| Generate Restart Points | Program Controlled |
| Retain Files After Full Solve | Yes |
| **Nonlinear Controls** | |
| Newton-Raphson Option | Program Controlled |
| Force Convergence | Program Controlled |
| Moment Convergence | Program Controlled |
| Displacement Convergence | Program Controlled |
| Rotation Convergence | Program Controlled |
| Line Search | Program Controlled |
| Stabilization | Off |
| **Output Controls** | |
| Stress | Yes |
| Strain | Yes |
| Nodal Forces | No |
| Contact Miscellaneous | No |
| General Miscellaneous | No |
| Store Results At | All Time Points |

| Analysis Data Management | |
|---|---|
| Solver Files Directory | C:\Users\Inspiron\Desktop\damini files2\basic part analysis\fgffgfg_files\dp0\SYS\MECH\ |
| Future Analysis | Prestressed analysis |
| Scratch Solver Files Directory | |
| Save MAPDL db | No |
| Delete Unneeded Files | Yes |
| Nonlinear Solution | No |
| Solver Units | Active System |
| Solver Unit System | nmm |

**TABLE 8**
**Model (A4, B4) > Static Structural (A5) > Loads**

| Object Name | *Fixed Support* | *Pressure* |
|---|---|---|
| State | Fully Defined | |
| **Scope** | | |
| Scoping Method | Geometry Selection | |
| Geometry | 1 Face | |
| **Definition** | | |
| Type | Fixed Support | Pressure |
| Suppressed | No | |
| Define By | | Normal To |
| Magnitude | | 1.02 MPa (ramped) |

**FIGURE 1**
**Model (A4, B4) > Static Structural (A5) > Pressure**

`

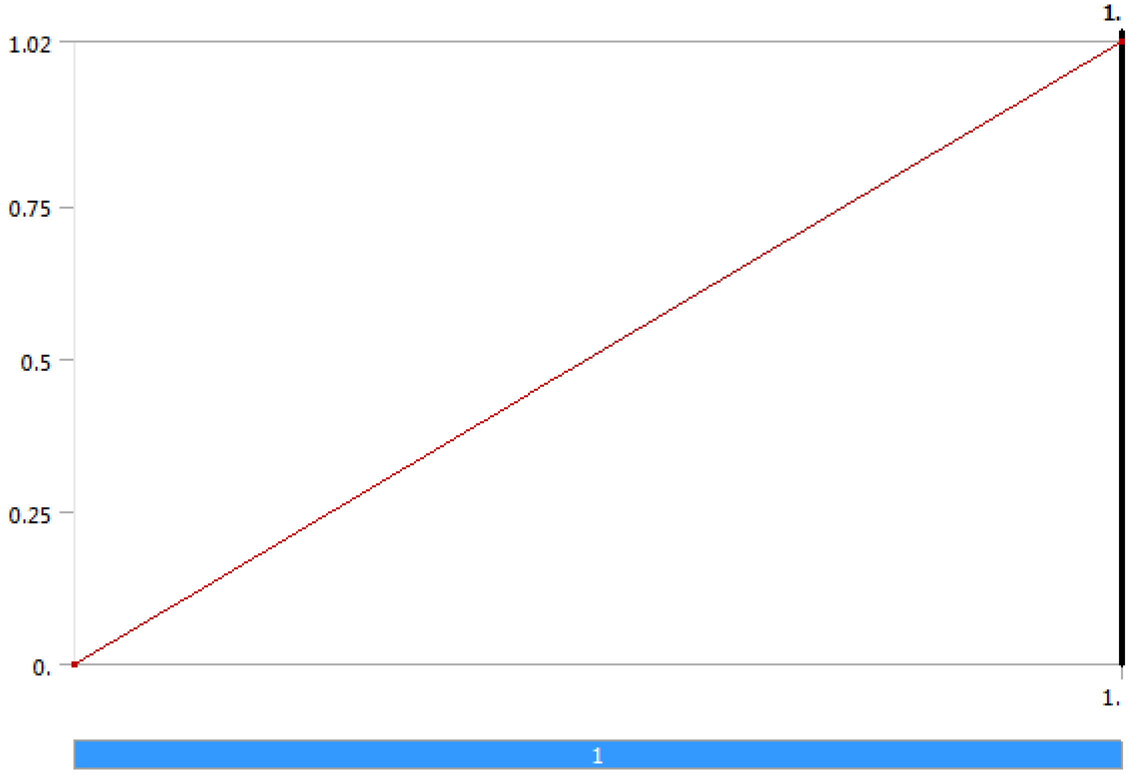


## Solution (A6)

**TABLE 9**
**Model (A4, B4) > Static Structural (A5) > Solution**

| | |
|---|---|
| Object Name | *Solution (A6)* |
| State | Solved |
| **Adaptive Mesh Refinement** | |
| Max Refinement Loops | 1. |
| Refinement Depth | 2. |
| **Information** | |
| Status | Done |

**TABLE 10**
**Model (A4, B4) > Static Structural (A5) > Solution (A6) > Solution Information**

| | |
|---|---|
| Object Name | *Solution Information* |
| State | Solved |
| **Solution Information** | |
| Solution Output | Solver Output |

`

| | |
|---|---|
| Newton-Raphson Residuals | 0 |
| Update Interval | 2.5 s |
| Display Points | All |
| **FE Connection Visibility** | |
| Activate Visibility | Yes |
| Display | All FE Connectors |
| Draw Connections Attached To | All Nodes |
| Line Color | Connection Type |
| Visible on Results | No |
| Line Thickness | Single |
| Display Type | Lines |

**TABLE 11**
**Model (A4, B4) > Static Structural (A5) > Solution (A6) > Results**

| Object Name | *Equivalent Stress* | *Maximum Principal Stress* | *Maximum Shear Stress* |
|---|---|---|---|
| State | Solved | | |
| **Scope** | | | |
| Scoping Method | Geometry Selection | | |
| Geometry | All Bodies | | |
| **Definition** | | | |
| Type | Equivalent (von-Mises) Stress | Maximum Principal Stress | Maximum Shear Stress |
| By | Time | | |
| Display Time | Last | | |
| Calculate Time History | Yes | | |
| Identifier | | | |
| Suppressed | No | | |
| **Integration Point Results** | | | |

`

| | | | |
|---|---|---|---|
| Display Option | Averaged | | |
| Average Across Bodies | No | | |
| **Results** | | | |
| Minimum | 8.6998e-003 MPa | -45.988 MPa | 4.79e-003 MPa |
| Maximum | 106.82 MPa | 160.27 MPa | 56.864 MPa |
| **Minimum Value Over Time** | | | |
| Minimum | 8.6998e-003 MPa | -45.988 MPa | 4.79e-003 MPa |
| Maximum | 8.6998e-003 MPa | -45.988 MPa | 4.79e-003 MPa |
| **Maximum Value Over Time** | | | |
| Minimum | 106.82 MPa | 160.27 MPa | 56.864 MPa |
| Maximum | 106.82 MPa | 160.27 MPa | 56.864 MPa |
| **Information** | | | |
| Time | 1. s | | |
| Load Step | 1 | | |
| Substep | 1 | | |
| Iteration Number | 1 | | |

## Linear Buckling (B5)

**TABLE 12**
**Model (A4, B4) > Analysis**

| | |
|---|---|
| Object Name | *Linear Buckling (B5)* |
| State | Solved |
| **Definition** | |
| Physics Type | Structural |
| Analysis Type | Linear Buckling |
| Solver Target | Mechanical APDL |
| **Options** | |
| Generate Input Only | No |

`

**TABLE 13**
**Model (A4, B4) > Linear Buckling (B5) > Initial Condition**

| | |
|---|---|
| Object Name | *Pre-Stress (Static Structural)* |
| State | Fully Defined |
| **Definition** | |
| Pre-Stress Environment | Static Structural |
| Pre-Stress Define By | Program Controlled |
| Reported Loadstep | Last |
| Reported Substep | Last |
| Reported Time | End Time |
| Contact Status | Use True Status |

**TABLE 14**
**Model (A4, B4) > Linear Buckling (B5) > Analysis Settings**

| | |
|---|---|
| Object Name | *Analysis Settings* |
| State | Fully Defined |
| **Options** | |
| Max Modes to Find | 2. |
| **Solver Controls** | |
| Solver Type | Program Controlled |
| **Output Controls** | |
| Stress | No |
| Strain | No |
| General Miscellaneous | No |
| **Analysis Data Management** | |
| Solver Files Directory | C:\Users\Inspiron\Desktop\damini files2\basic part analysis\fgffgfg_files\dp0\SYS-1\MECH\ |
| Future Analysis | None |
| Scratch Solver Files Directory | |

`

| | |
|---|---|
| Save MAPDL db | No |
| Delete Unneeded Files | Yes |
| Solver Units | Active System |
| Solver Unit System | nmm |

## Solution (B6)

**TABLE 15**
**Model (A4, B4) > Linear Buckling (B5) > Solution**

| | |
|---|---|
| Object Name | *Solution (B6)* |
| State | Solved |
| **Adaptive Mesh Refinement** | |
| Max Refinement Loops | 1. |
| Refinement Depth | 2. |
| **Information** | |
| Status | Done |

**FIGURE 2**
**Model (A4, B4) > Linear Buckling (B5) > Solution (B6)**

`

**TABLE 16**
**Model (A4, B4) > Linear Buckling (B5) > Solution (B6)**

| Mode | Load Multiplier |
|---|---|
| 1. | 6.7277 |
| 2. | 14.126 |

**TABLE 17**
**Model (A4, B4) > Linear Buckling (B5) > Solution (B6) > Solution Information**

| | |
|---|---|
| Object Name | *Solution Information* |
| State | Solved |
| **Solution Information** | |
| Solution Output | Solver Output |
| Newton-Raphson Residuals | 0 |
| Update Interval | 2.5 s |
| Display Points | All |
| **FE Connection Visibility** | |
| Activate Visibility | Yes |
| Display | All FE Connectors |
| Draw Connections Attached To | All Nodes |
| Line Color | Connection Type |
| Visible on Results | No |
| Line Thickness | Single |
| Display Type | Lines |

**TABLE 18**
**Model (A4, B4) > Linear Buckling (B5) > Solution (B6) > Results**

| | |
|---|---|
| Object Name | *Total Deformation* |
| State | Solved |
| **Scope** | |
| Scoping Method | Geometry Selection |
| Geometry | All Bodies |

`

| Definition | |
|---|---|
| Type | Total Deformation |
| Mode | 1. |
| Identifier | |
| Suppressed | No |
| **Results** | |
| Load Multiplier | 6.7277 |
| Minimum | 0. mm |
| Maximum | 1.0076 mm |
| **Minimum Value Over Time** | |
| Minimum | 0. mm |
| Maximum | 0. mm |
| **Maximum Value Over Time** | |
| Minimum | 1.0076 mm |
| Maximum | 1.0076 mm |

**TABLE 19**
**Model (A4, B4) > Linear Buckling (B5) > Solution (B6) > Total Deformation**

| Mode | Load Multiplier |
|---|---|
| 1. | 6.7277 |
| 2. | 14.126 |

# Material Data

## Structural Steel

**TABLE 20**
**Structural Steel > Constants**

| | |
|---|---|
| Density | 7.85e-006 kg mm^-3 |
| Coefficient of Thermal Expansion | 1.2e-005 C^-1 |
| Specific Heat | 4.34e+005 mJ kg^-1 C^-1 |
| Thermal Conductivity | 6.05e-002 W mm^-1 C^-1 |

`

| | |
|---|---|
| Resistivity | 1.7e-004 ohm mm |

**TABLE 21**
**Structural Steel > Compressive Ultimate Strength**

| Compressive Ultimate Strength MPa |
|---|
| 0 |

**TABLE 22**
**Structural Steel > Compressive Yield Strength**

| Compressive Yield Strength MPa |
|---|
| 250 |

**TABLE 23**
**Structural Steel > Tensile Yield Strength**

| Tensile Yield Strength MPa |
|---|
| 250 |

**TABLE 24**
**Structural Steel > Tensile Ultimate Strength**

| Tensile Ultimate Strength MPa |
|---|
| 460 |

**TABLE 25**
**Structural Steel > Isotropic Secant Coefficient of Thermal Expansion**

| Reference Temperature C |
|---|
| 22 |

**TABLE 26**
**Structural Steel > Alternating Stress Mean Stress**

| Alternating Stress MPa | Cycles | Mean Stress MPa |
|---|---|---|
| 3999 | 10 | 0 |
| 2827 | 20 | 0 |
| 1896 | 50 | 0 |
| 1413 | 100 | 0 |
| 1069 | 200 | 0 |
| 441 | 2000 | 0 |

`

| | | |
|---|---|---|
| 262 | 10000 | 0 |
| 214 | 20000 | 0 |
| 138 | 1.e+005 | 0 |
| 114 | 2.e+005 | 0 |
| 86.2 | 1.e+006 | 0 |

**TABLE 27**
**Structural Steel > Strain-Life Parameters**

| Strength Coefficient MPa | Strength Exponent | Ductility Coefficient | Ductility Exponent | Cyclic Strength Coefficient MPa | Cyclic Strain Hardening Exponent |
|---|---|---|---|---|---|
| 920 | -0.106 | 0.213 | -0.47 | 1000 | 0.2 |

**TABLE 28**
**Structural Steel > Isotropic Elasticity**

| Temperature C | Young's Modulus MPa | Poisson's Ratio | Bulk Modulus MPa | Shear Modulus MPa |
|---|---|---|---|---|
| | 2.e+005 | 0.3 | 1.6667e+005 | 76923 |

**TABLE 29**
**Structural Steel > Isotropic Relative Permeability**

| Relative Permeability |
|---|
| 10000 |

`

# APPENDIX B

ANSYS report file of the corrugated beam (model 13):

Project

| | |
|---|---|
| First Saved | Tuesday, March 27, 2018 |
| Last Saved | Saturday, May 05, 2018 |
| Product Version | 15.0 Release |
| Save Project Before Solution | No |
| Save Project After Solution | No |

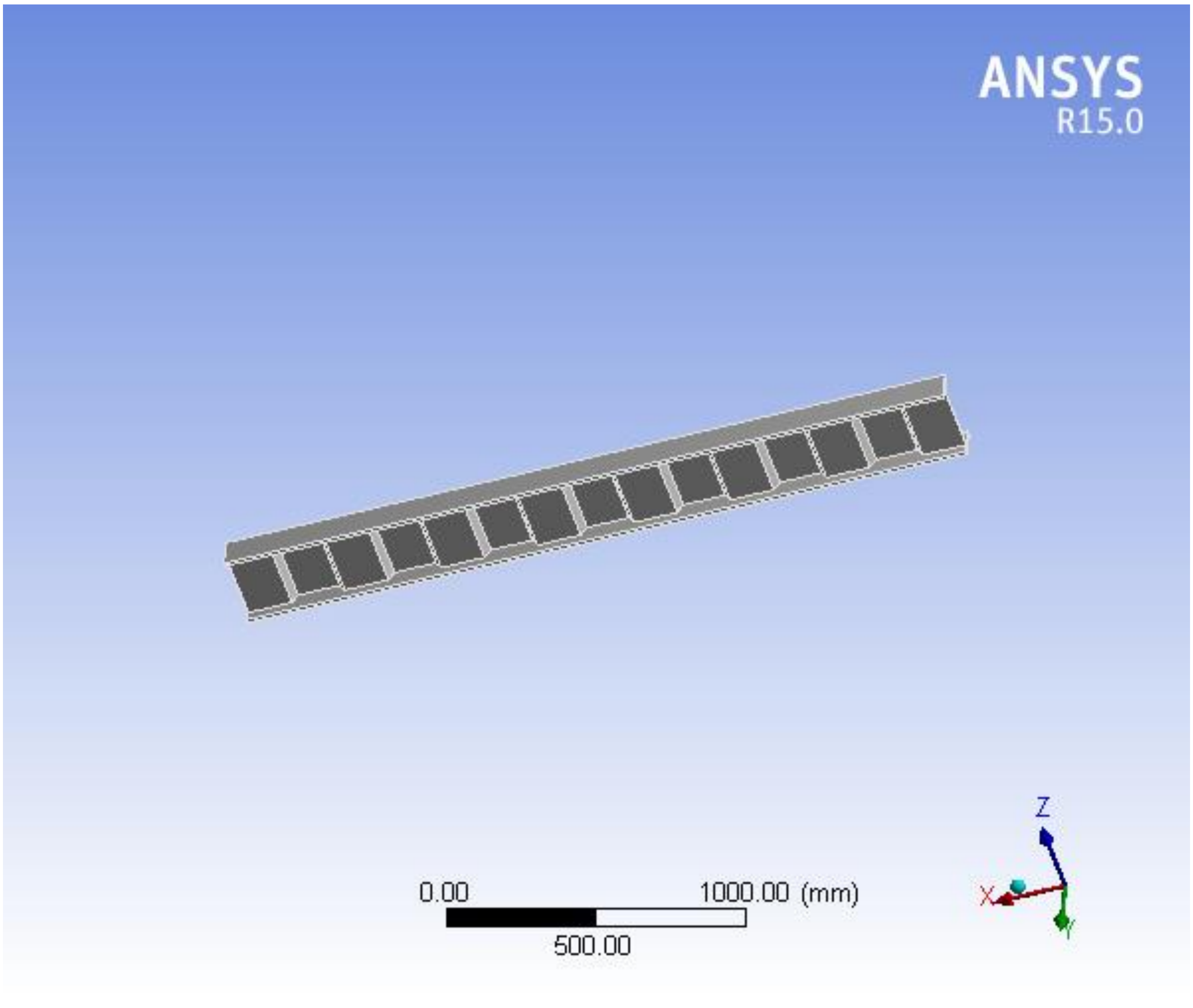

`

## Contents



## Units

**TABLE 1**

| | |
|---|---|
| Unit System | Metric (mm, kg, N, s, mV, mA) Degrees rad/s Celsius |
| Angle | Degrees |
| Rotational Velocity | rad/s |
| Temperature | Celsius |

## Model (A4, B4)

### Geometry

**TABLE 2**
**Model (A4, B4) > Geometry**

| | |
|---|---|
| Object Name | *Geometry* |
| State | Fully Defined |
| **Definition** | |
| Source | D:\udl analysis\part 13 udl_files\dp0\SYS\DM\SYS.agdb |
| Type | DesignModeler |

`

| | |
|---|---|
| Length Unit | Meters |
| Element Control | Program Controlled |
| Display Style | Body Color |
| **Bounding Box** | |
| Length X | 2540. mm |
| Length Y | 118. mm |
| Length Z | 254. mm |
| **Properties** | |
| Volume | 1.1379e+007 $mm^3$ |
| Mass | 89.325 kg |
| Scale Factor Value | 1. |
| **Statistics** | |
| Bodies | 1 |
| Active Bodies | 1 |
| Nodes | 62082 |
| Elements | 30536 |
| Mesh Metric | None |
| **Basic Geometry Options** | |
| Parameters | Yes |
| Parameter Key | DS |
| Attributes | No |
| Named Selections | No |
| Material Properties | No |
| **Advanced Geometry Options** | |
| Use Associativity | Yes |
| Coordinate Systems | No |
| Reader Mode Saves Updated File | No |

`

| | |
|---|---|
| Use Instances | Yes |
| Smart CAD Update | No |
| Compare Parts On Update | No |
| Attach File Via Temp File | Yes |
| Temporary Directory | C:\Users\Inspiron\AppData\Roaming\Ansys\v150 |
| Analysis Type | 3-D |
| Decompose Disjoint Geometry | Yes |
| Enclosure and Symmetry Processing | Yes |

**TABLE 3**
**Model (A4, B4) > Geometry > Parts**

| | |
|---|---|
| Object Name | *SURF* |
| State | Meshed |
| **Graphics Properties** | |
| Visible | Yes |
| Transparency | 1 |
| **Definition** | |
| Suppressed | No |
| Stiffness Behavior | Flexible |
| Coordinate System | Default Coordinate System |
| Reference Temperature | By Environment |
| **Material** | |
| Assignment | Structural Steel |
| Nonlinear Effects | Yes |
| Thermal Strain Effects | Yes |
| **Bounding Box** | |
| Length X | 2540. mm |
| Length Y | 118. mm |

`

| | |
|---|---|
| Length Z | 254. mm |
| **Properties** | |
| Volume | 1.1379e+007 mm³ |
| Mass | 89.325 kg |
| Centroid X | 1270.8 mm |
| Centroid Y | 0.33689 mm |
| Centroid Z | 127. mm |
| Moment of Inertia Ip1 | 1.0681e+006 kg·mm² |
| Moment of Inertia Ip2 | 4.8874e+007 kg·mm² |
| Moment of Inertia Ip3 | 4.7959e+007 kg·mm² |
| **Statistics** | |
| Nodes | 62082 |
| Elements | 30536 |
| Mesh Metric | None |

## Coordinate Systems

**TABLE 4**
**Model (A4, B4) > Coordinate Systems > Coordinate System**

| | |
|---|---|
| Object Name | *Global Coordinate System* |
| State | Fully Defined |
| **Definition** | |
| Type | Cartesian |
| Coordinate System ID | 0. |
| **Origin** | |
| Origin X | 0. mm |
| Origin Y | 0. mm |
| Origin Z | 0. mm |
| **Directional Vectors** | |

`

| | |
|---|---|
| X Axis Data | [ 1. 0. 0. ] |
| Y Axis Data | [ 0. 1. 0. ] |
| Z Axis Data | [ 0. 0. 1. ] |

## Mesh

**TABLE 5**
**Model (A4, B4) > Mesh**

| | |
|---|---|
| Object Name | *Mesh* |
| State | Solved |
| **Defaults** | |
| Physics Preference | Mechanical |
| Relevance | 0 |
| **Sizing** | |
| Use Advanced Size Function | Off |
| Relevance Center | Coarse |
| Element Size | 10.0 mm |
| Initial Size Seed | Active Assembly |
| Smoothing | Medium |
| Transition | Fast |
| Span Angle Center | Coarse |
| Minimum Edge Length | 7.33180 mm |
| **Inflation** | |
| Use Automatic Inflation | None |
| Inflation Option | Smooth Transition |
| Transition Ratio | 0.272 |
| Maximum Layers | 5 |
| Growth Rate | 1.2 |
| Inflation Algorithm | Pre |

`

| | |
|---|---|
| View Advanced Options | No |
| **Patch Conforming Options** | |
| Triangle Surface Mesher | Program Controlled |
| **Patch Independent Options** | |
| Topology Checking | Yes |
| **Advanced** | |
| Number of CPUs for Parallel Part Meshing | Program Controlled |
| Shape Checking | Standard Mechanical |
| Element Midside Nodes | Program Controlled |
| Straight Sided Elements | No |
| Number of Retries | Default (4) |
| Extra Retries For Assembly | Yes |
| Rigid Body Behavior | Dimensionally Reduced |
| Mesh Morphing | Disabled |
| **Defeaturing** | |
| Pinch Tolerance | Please Define |
| Generate Pinch on Refresh | No |
| Automatic Mesh Based Defeaturing | On |
| Defeaturing Tolerance | Default |
| **Statistics** | |
| Nodes | 62082 |
| Elements | 30536 |
| Mesh Metric | None |

## Static Structural (A5)

**TABLE 6**
**Model (A4, B4) > Analysis**

| | |
|---|---|
| Object Name | *Static Structural (A5)* |

`

| | |
|---|---|
| State | Solved |
| **Definition** | |
| Physics Type | Structural |
| Analysis Type | Static Structural |
| Solver Target | Mechanical APDL |
| **Options** | |
| Environment Temperature | 22. °C |
| Generate Input Only | No |

**TABLE 7**
**Model (A4, B4) > Static Structural (A5) > Analysis Settings**

| | |
|---|---|
| Object Name | *Analysis Settings* |
| State | Fully Defined |
| **Restart Analysis** | |
| Restart Type | Program Controlled |
| Status | Done |
| **Step Controls** | |
| Number Of Steps | 1. |
| Current Step Number | 1. |
| Step End Time | 1. s |
| Auto Time Stepping | Program Controlled |
| **Solver Controls** | |
| Solver Type | Program Controlled |
| Weak Springs | Program Controlled |
| Large Deflection | Off |
| Inertia Relief | Off |
| **Restart Controls** | |
| Generate Restart Points | Program Controlled |

`

| | |
|---|---|
| Retain Files After Full Solve | Yes |
| **Nonlinear Controls** | |
| Newton-Raphson Option | Program Controlled |
| Force Convergence | Program Controlled |
| Moment Convergence | Program Controlled |
| Displacement Convergence | Program Controlled |
| Rotation Convergence | Program Controlled |
| Line Search | Program Controlled |
| Stabilization | Off |
| **Output Controls** | |
| Stress | Yes |
| Strain | Yes |
| Nodal Forces | No |
| Contact Miscellaneous | No |
| General Miscellaneous | No |
| Store Results At | All Time Points |
| **Analysis Data Management** | |
| Solver Files Directory | D:\udl analysis\part 13 udl_files\dp0\SYS\MECH\ |
| Future Analysis | Prestressed analysis |
| Scratch Solver Files Directory | |
| Save MAPDL db | No |
| Delete Unneeded Files | Yes |
| Nonlinear Solution | No |
| Solver Units | Active System |
| Solver Unit System | nmm |

**TABLE 8**
**Model (A4, B4) > Static Structural (A5) > Loads**

`

| Object Name | *Pressure* | *Fixed Support* |
|---|---|---|
| State | Fully Defined | |
| **Scope** | | |
| Scoping Method | Geometry Selection | |
| Geometry | 1 Face | |
| **Definition** | | |
| Type | Pressure | Fixed Support |
| Define By | Normal To | |
| Magnitude | 1.02 MPa (ramped) | |
| Suppressed | No | |

**FIGURE 1**
**Model (A4, B4) > Static Structural (A5) > Pressure**

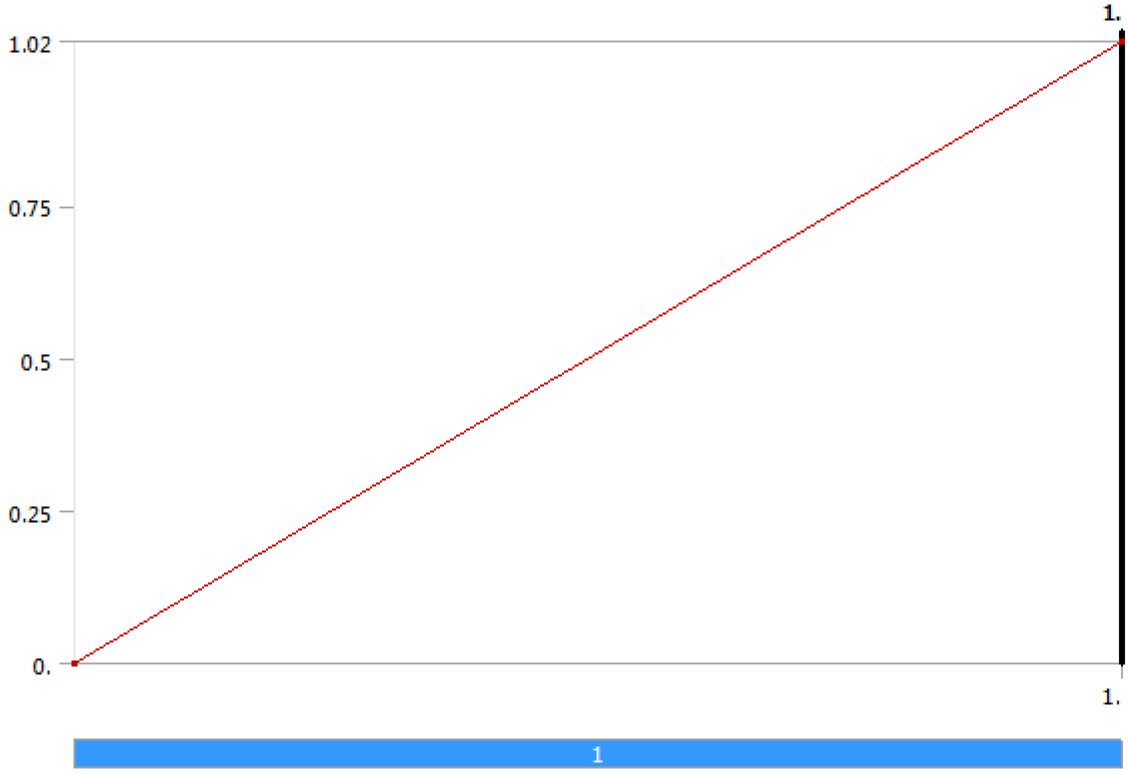


## Solution (A6)

**TABLE 9**
**Model (A4, B4) > Static Structural (A5) > Solution**

| Object Name | *Solution (A6)* |
|---|---|

`

| | |
|---|---|
| State | Solved |
| **Adaptive Mesh Refinement** | |
| Max Refinement Loops | 1. |
| Refinement Depth | 2. |
| **Information** | |
| Status | Done |

**TABLE 10**
**Model (A4, B4) > Static Structural (A5) > Solution (A6) > Solution Information**

| | |
|---|---|
| Object Name | *Solution Information* |
| State | Solved |
| **Solution Information** | |
| Solution Output | Solver Output |
| Newton-Raphson Residuals | 0 |
| Update Interval | 2.5 s |
| Display Points | All |
| **FE Connection Visibility** | |
| Activate Visibility | Yes |
| Display | All FE Connectors |
| Draw Connections Attached To | All Nodes |
| Line Color | Connection Type |
| Visible on Results | No |
| Line Thickness | Single |
| Display Type | Lines |

**TABLE 11**
**Model (A4, B4) > Static Structural (A5) > Solution (A6) > Results**

| Object Name | *Total Deformation* | *Directional Deformation* | *Directional Deformation 2* | *Directional Deformation 3* | *Equivalent Elastic Strain* | *Equivalent Stress* | *Maximum Principal Stress* | *Maximum Shear Stress* |
|---|---|---|---|---|---|---|---|---|

| | | | | | | |
|---|---|---|---|---|---|---|
| State | Solved | | | | | |
| **Scope** | | | | | | |
| Scoping Method | Geometry Selection | | | | | |
| Geometry | All Bodies | | | | | |
| **Definition** | | | | | | |
| Type | Total Deformation | Directional Deformation | Equivalent Elastic Strain | Equivalent (von-Mises) Stress | Maximum Principal Stress | Maximum Shear Stress |
| By | Time | | | | | |
| Display Time | Last | | | | | |
| Calculate Time History | Yes | | | | | |
| Identifier | | | | | | |
| Suppressed | No | | | | | |
| Orientation | | X Axis | | | | |
| Coordinate System | | Global Coordinate System | | | | |
| **Results** | | | | | | |
| Minimum | 0. mm | -0.51865 mm | 1.1062e-007 mm/mm | 2.2123e-002 MPa | -49.94 MPa | 1.2304e-002 MPa |
| Maximum | 7.518 mm | 0.53235 mm | 8.0589e-004 mm/mm | 106.61 MPa | 155.00 MPa | 55.34 MPa |
| **Minimum Value Over Time** | | | | | | |
| Minimum | 0. mm | -0.51865 mm | 1.1062e-007 mm/mm | 2.2123e-002 MPa | -49.94 MPa | 1.2304e-002 MPa |

`

| | | | | | | |
|---|---|---|---|---|---|---|
| Maximum | 0. mm | -0.51865 mm | 1.1062e-007 mm/mm | 2.2123e-002 MPa | -49.94 MPa | 1.2304e-002 MPa |
| **Maximum Value Over Time** | | | | | | |
| Minimum | 7.518 mm | 0.53235 mm | 8.0589e-004 mm/mm | 106.61 MPa | 155.00 MPa | 55.34 MPa |
| Maximum | 7.518 mm | 0.53235 mm | 8.0589e-004 mm/mm | 106.61 MPa | 155.00 MPa | 55.34 MPa |
| **Information** | | | | | | |
| Time | 1. s | | | | | |
| Load Step | 1 | | | | | |
| Substep | 1 | | | | | |
| Iteration Number | 1 | | | | | |
| **Integration Point Results** | | | | | | |
| Display Option | | | Averaged | | | |
| Average Across Bodies | | | No | | | |

## Linear Buckling (B5)

**TABLE 12**
**Model (A4, B4) > Analysis**

| | |
|---|---|
| Object Name | *Linear Buckling (B5)* |
| State | Solved |
| **Definition** | |
| Physics Type | Structural |
| Analysis Type | Linear Buckling |
| Solver Target | Mechanical APDL |
| **Options** | |

`

| | |
|---|---|
| Generate Input Only | No |

**TABLE 13**
**Model (A4, B4) > Linear Buckling (B5) > Initial Condition**

| | |
|---|---|
| Object Name | *Pre-Stress (Static Structural)* |
| State | Fully Defined |
| **Definition** | |
| Pre-Stress Environment | Static Structural |
| Pre-Stress Define By | Program Controlled |
| Reported Loadstep | Last |
| Reported Substep | Last |
| Reported Time | End Time |
| Contact Status | Use True Status |

**TABLE 14**
**Model (A4, B4) > Linear Buckling (B5) > Analysis Settings**

| | |
|---|---|
| Object Name | *Analysis Settings* |
| State | Fully Defined |
| **Options** | |
| Max Modes to Find | 2. |
| **Solver Controls** | |
| Solver Type | Program Controlled |
| **Output Controls** | |
| Stress | No |
| Strain | No |
| General Miscellaneous | No |
| **Analysis Data Management** | |
| Solver Files Directory | D:\udl analysis\part 13 udl_files\dp0\SYS-1\MECH\ |
| Future Analysis | None |
| Scratch Solver Files Directory | |

`

| | |
|---|---|
| Save MAPDL db | No |
| Delete Unneeded Files | Yes |
| Solver Units | Active System |
| Solver Unit System | nmm |

## Solution (B6)

**TABLE 15**
**Model (A4, B4) > Linear Buckling (B5) > Solution**

| | |
|---|---|
| Object Name | *Solution (B6)* |
| State | Solved |
| **Adaptive Mesh Refinement** | |
| Max Refinement Loops | 1. |
| Refinement Depth | 2. |
| **Information** | |
| Status | Done |

**FIGURE 2**
**Model (A4, B4) > Linear Buckling (B5) > Solution (B6)**

`

**TABLE 16**
**Model (A4, B4) > Linear Buckling (B5) > Solution (B6)**

| Mode | Load Multiplier |
|---|---|
| 1. | 7.4848 |
| 2. | 17.469 |

**TABLE 17**
**Model (A4, B4) > Linear Buckling (B5) > Solution (B6) > Solution Information**

| Object Name | *Solution Information* |
|---|---|
| State | Solved |
| **Solution Information** | |
| Solution Output | Solver Output |
| Newton-Raphson Residuals | 0 |
| Update Interval | 2.5 s |
| Display Points | All |
| **FE Connection Visibility** | |
| Activate Visibility | Yes |
| Display | All FE Connectors |
| Draw Connections Attached To | All Nodes |
| Line Color | Connection Type |
| Visible on Results | No |
| Line Thickness | Single |
| Display Type | Lines |

**TABLE 18**
**Model (A4, B4) > Linear Buckling (B5) > Solution (B6) > Results**

| Object Name | *Total Deformation* | *Total Deformation 2* | *Directional Deformation* | *Directional Deformation 2* |
|---|---|---|---|---|
| State | Solved | | | |
| **Scope** | | | | |
| Scoping Method | Geometry Selection | | | |

`

| | | | | |
|---|---|---|---|---|
| Geometry | All Bodies | | | |
| **Definition** | | | | |
| Type | Total Deformation | | Directional Deformation | |
| Mode | 1. | 2. | 1. | 2. |
| Identifier | | | | |
| Suppressed | No | | | |
| Orientation | | | Y Axis | |
| Coordinate System | | | Global Coordinate System | |
| **Results** | | | | |
| Load Multiplier | 7.4848 | 17.469 | 7.4848 | 17.469 |
| Minimum | 0. mm | | -2.791e-005 mm | -0.34685 mm |
| Maximum | 1.0093 mm | 1.0045 mm | 1. mm | |
| **Minimum Value Over Time** | | | | |
| Minimum | 0. mm | | -2.791e-005 mm | -0.34685 mm |
| Maximum | 0. mm | | -2.791e-005 mm | -0.34685 mm |
| **Maximum Value Over Time** | | | | |
| Minimum | 1.0093 mm | 1.0045 mm | 1. mm | |
| Maximum | 1.0093 mm | 1.0045 mm | 1. mm | |

**TABLE 19**
**Model (A4, B4) > Linear Buckling (B5) > Solution (B6) > Total Deformation**

| Mode | Load Multiplier |
|---|---|
| 1. | 7.4848 |
| 2. | 17.469 |

**TABLE 20**
**Model (A4, B4) > Linear Buckling (B5) > Solution (B6) > Total Deformation 2**

| Mode | Load Multiplier |
|---|---|
| 1. | 7.4848 |

`

| | |
|---|---|
| 2. | 17.469 |

**TABLE 21**
**Model (A4, B4) > Linear Buckling (B5) > Solution (B6) > Directional Deformation**

| Mode | Load Multiplier |
|---|---|
| 1. | 7.4848 |
| 2. | 17.469 |

**TABLE 22**
**Model (A4, B4) > Linear Buckling (B5) > Solution (B6) > Directional Deformation 2**

| Mode | Load Multiplier |
|---|---|
| 1. | 7.4848 |
| 2. | 17.469 |

## Material Data

### Structural Steel

**TABLE 23**
**Structural Steel > Constants**

| | |
|---|---|
| Density | 7.85e-006 kg mm^-3 |
| Coefficient of Thermal Expansion | 1.2e-005 C^-1 |
| Specific Heat | 4.34e+005 mJ kg^-1 C^-1 |
| Thermal Conductivity | 6.05e-002 W mm^-1 C^-1 |
| Resistivity | 1.7e-004 ohm mm |

**TABLE 24**
**Structural Steel > Compressive Ultimate Strength**

| Compressive Ultimate Strength MPa |
|---|
| 0 |

**TABLE 25**
**Structural Steel > Compressive Yield Strength**

| Compressive Yield Strength MPa |
|---|
| 250 |

**TABLE 26**
**Structural Steel > Tensile Yield Strength**

`

| Tensile Yield Strength MPa |
|---|
| 250 |

**TABLE 27**
**Structural Steel > Tensile Ultimate Strength**

| Tensile Ultimate Strength MPa |
|---|
| 460 |

**TABLE 28**
**Structural Steel > Isotropic Secant Coefficient of Thermal Expansion**

| Reference Temperature C |
|---|
| 22 |

**TABLE 29**
**Structural Steel > Alternating Stress Mean Stress**

| Alternating Stress MPa | Cycles | Mean Stress MPa |
|---|---|---|
| 3999 | 10 | 0 |
| 2827 | 20 | 0 |
| 1896 | 50 | 0 |
| 1413 | 100 | 0 |
| 1069 | 200 | 0 |
| 441 | 2000 | 0 |
| 262 | 10000 | 0 |
| 214 | 20000 | 0 |
| 138 | 1.e+005 | 0 |
| 114 | 2.e+005 | 0 |
| 86.2 | 1.e+006 | 0 |

**TABLE 30**
**Structural Steel > Strain-Life Parameters**

| Strength Coefficient MPa | Strength Exponent | Ductility Coefficient | Ductility Exponent | Cyclic Strength Coefficient MPa | Cyclic Strain Hardening Exponent |
|---|---|---|---|---|---|
| 920 | -0.106 | 0.213 | -0.47 | 1000 | 0.2 |

`

**TABLE 31**
**Structural Steel > Isotropic Elasticity**

| Temperature C | Young's Modulus MPa | Poisson's Ratio | Bulk Modulus MPa | Shear Modulus MPa |
|---|---|---|---|---|
| | 2.e+005 | 0.3 | 1.6667e+005 | 76923 |

**TABLE 32**
**Structural Steel > Isotropic Relative Permeability**

| Relative Permeability |
|---|
| 10000 |

# JAYPEE UNIVERSITY OF INFORMATION TECHNOLOGY, WAKNAGHAT
## LEARNING RESOURCE CENTER

## PLAGIARISM VERIFICATION REPORT

**Date:** 9/5/18

**Type of Document (Tick):** Thesis | M.Tech Dissertation/ Report ✓ | B.Tech Project Report | Paper

**Name:** DAMINI TALWAR **Department:** CIVIL ENGINEERING

**Enrolment No.** 162660 **Registration No.** 162660

**Phone No.** 9805391360 **Email ID.** sweet.dami123@gmail.com

**Name of the Supervisor:** DR. SAURAV

**Title of the Thesis/Dissertation/Project Report/Paper (In Capital letters):** FINITE ELEMENT ANALYSIS OF A BEAM WITH CORRUGATED WEB OF A JIB CRANE

Kindly allow me to avail Turnitin software report for the document mentioned above.

Damini
(Signature)

**FOR ACCOUNTS DEPARTMENT:**

Five hundred only

Amount deposited: Rs. 500/- Dated: 9/5/18 Receipt No. Bsm1005/226
(Enclosed payment slip)

(Account Officer)

**FOR LRC USE:**
The above document was scanned for plagiarism check. The outcome of the same is reported below:

| Copy Received on | Report delivered on | Similarity Index in % | Submission Details | |
|---|---|---|---|---|
| 09/05/2018 | 09/05/2018 | 21% | Word Counts | 16,795 |
| | | | Character Counts | 83,630 |
| | | | Page counts | 94 |
| | | | File Size | 2.61M |

Checked by
Name & Signature

Librarian

turnitin

# Digital Receipt

This receipt acknowledges that Turnitin received your paper. Below you will find the receipt information regarding your submission.

The first page of your submissions is displayed below.

| | |
|---|---|
| Submission author: | Damini Talwar |
| Assignment title: | MTech Project Reports |
| Submission title: | FINITE ELEMENT ANALYSIS OF A B.. |
| File name: | M.Tech_Damini_162660.pdf |
| File size: | 2.61M |
| Page count: | 94 |
| Word count: | 16,795 |
| Character count: | 83,630 |
| Submission date: | 09-May-2018 01:51PM (UTC+0530) |
| Submission ID: | 961250452 |

FINITE ELEMENT ANALYSIS OF A BEAM WITH
CORRUGATED WEB OF A JIB CRANE

A Thesis

*Submitted in partial fulfillment of the requirements for the award of the degree*

*of*

MASTER OF TECHNOLOGY

IN

CIVIL ENGINEERING

With specialization in

STRUCTURAL ENGINEERING

*Under the supervision of*

Dr. Saurav
(Assistant Professor)

*by*

DAMINI TALWAR
Roll No. 162660

To

Juit

JAYPEE UNIVERSITY OF INFORMATION TECHNOLOGY
WAKNAGHAT, SOLAN – 173234
HIMACHAL PRADESH, INDIA
May 2018